

Supplementary Material

QSAR and Molecular Docking Studies of the Inhibitory Activity of Novel Heterocyclic GABA Analogues over GABA-AT

Josué Rodríguez-Lozada¹, Erika Tovar-Gudiño¹, Juan Alberto Guevara-Salazar², Rodrigo Said Razo-Hernández³, Ángel Santiago³, Nina Pastor³, Mario Fernández-Zertuche^{1*}

Table of Contents

NMR Data for analogues 7, 8 and 9	08
Computational Details	24
NMR Data for analogues 7, 8 and 9	
Figure 1S. ¹ H NMR (200 MHz, CD ₃ OD) of 4-(thiazolidin-3-yl)butanoic acid (7a)	06
Figure 2S. ¹³ C NMR (50 MHz, CD ₃ OD) of 4-(thiazolidin-3-yl)butanoic acid (7a)	06
Figure 3S. ¹ H NMR (400 MHz, CD ₃ OD) of 4-(piperidin-1-yl)butanoic acid (7b).	07
Figure 4S. ¹³ C NMR (400 MHz, CD ₃ OD) of 4-(piperidin-1-yl)butanoic acid (7b).	07
Figure 5S. ¹ H NMR (400 MHz, D ₂ O) of 4-(3-methylpiperidin-1-yl)butanoic acid (7c)	07
Figure 6S. ¹³ C NMR (100 MHz, D ₂ O) of sodium 4-(3-methylpiperidin-1-yl)butanoic acid (7c).	08
Figure 7S. ¹ H NMR (400 MHz, CD ₃ OD) of 4-(4-methylpiperidin-1-yl)butanoic acid (7d).	08
Figure 8S. ¹³ C NMR (100 MHz, CD ₃ OD) of 4-(4-methylpiperidin-1-yl)butanoic acid (7d).	08
Figure 9S. ¹ H NMR (400 MHz, CD ₃ OD) of 4-morpholinobutanoic acid (7e).	09
Figure 10S. ¹³ C NMR (100 MHz, CD ₃ OD) of	09

4-morpholinobutanoic acid (**7e**).

Figure 11S. ¹H NMR (400 MHz, CD₃OD) of 4-thiomorpholinobutanoic acid (**7f**). 09

Figure 12S. ¹³C NMR (100 MHz, CD₃OD) of 4-thiomorpholinobutanoic acid (**7f**). 10

Figure 13S. ¹H NMR (400 MHz, CD₃OD) of 5-methyl-3-(thiazolidin-3-ylmethyl)hexanoic acid (**8a**). 10

Figure 14S. ¹³C NMR (100 MHz, CD₃OD) of 5-methyl-3-(thiazolidin-3-ylmethyl)hexanoic acid (**8a**). 10

Figure 15S. 2D NMR (HETCOR 400 MHz, CD₃OD) of 5-methyl-3-(thiazolidin-3-ylmethyl)hexanoic acid (**8a**). 11

Figure 16S. ¹H NMR (400 MHz, CD₃OD) of 5-methyl-3-(piperidin-1-ylmethyl)hexanoic acid (**8b**). 11

Figure 17S. ¹³C NMR (100 MHz, CD₃OD) of 5-methyl-3-(piperidin-1-ylmethyl)hexanoic acid (**8b**). 12

Figure 18S. 2D NMR (HETCOR 400 MHz, CD₃OD) of 5-methyl-3-(piperidina-1-ylmethyl) hexanoic acid (**8b**). 12

Figure 19S. ¹H NMR (400 MHz, CD₃OD) of 5-methyl-3-((3-methylpiperidin-1-yl)methyl)hexanoic acid (**8c**). 13

Figure 20S. ¹³C NMR (100 MHz, CD₃OD) of 5-methyl-3-((3-methylpiperidin-1-yl)methyl)hexanoic acid (**8c**). 13

Figure 21S. 2D NMR (HETCOR 400 MHz, CD₃OD) of 5-methyl-3-((3-methylpiperidin-1-yl)methyl)hexanoic acid (**8c**). 14

Figure 22S. ¹H NMR (400 MHz, CD₃OD) of 5-methyl-3-((4-methylpiperidin-1-yl)methyl)hexanoic acid (**8d**). 14

Figure 23S. ¹³C NMR (100 MHz, CD₃OD) of 5-methyl-3-((4-methylpiperidin-1-yl)methyl)hexanoic acid (**8d**). 15

Figure 24S. 2D NMR (HETCOR 400 MHz, CD₃OD) of 5-methyl-3-((4-methylpiperidin-1-yl)methyl)hexanoic acid (**8d**). 16

Figure 25S. ¹ H NMR (400 MHz, CD ₃ OD) of 5-methyl-3-(morpholinomethyl)hexanoic acid (8e).	16
Figure 26S. ¹³ C NMR (100 MHz, CD ₃ OD) of 5-methyl-3-(morpholinomethyl)hexanoic acid (8e).	17
Figure 27S. ¹ H NMR (400 MHz, CD ₃ OD) of 5-methyl-3-(thiomorpholinomethyl)hexanoic acid (8e).	17
Figure 28S. ¹³ C NMR (100 MHz, CD ₃ OD) of 5-methyl-3-(thiomorpholinomethyl)hexanoic acid (8f).	18
Figure 29S. ¹ H NMR (400 MHz, CD ₃ OD) of 3-(4-chlorophenyl)-4-(piperidin-1-yl)butanoic acid (9b).	18
Figure 30S. ¹³ C NMR (100 MHz, CD ₃ OD) of 3-(4-chlorophenyl)-4-(piperidin-1-yl)butanoic acid (9b).	18
Figure 31S. ¹ H NMR (400 MHz, CD ₃ OD) of 3-(4-chlorophenyl)-4-(3-methylpiperidin-1-yl)butanoic acid (9c).	19
Figure 32S. ¹³ C NMR (100 MHz, CD ₃ OD) of 3-(4-chlorophenyl)-4-(3-methylpiperidin-1-yl)butanoic acid (9c).	19
Figure 33S. ¹ H NMR (400 MHz, CD ₃ OD) of 3-(4-chlorophenyl)-4-(4-methylpiperidin-1-yl) butanoic acid (9d).	19
Figure 34S. ¹³ C NMR (100 MHz, CD ₃ OD) of 3-(4-chlorophenyl)-4-(4-methylpiperidin-1-yl) butanoic acid (9d).	20
Figure 35S. 2D NMR (HETCOR 400 MHz, CD ₃ OD) of 3-(4-chlorophenyl)-4-(4-methylpiperidin-1-yl)butanoic acid (9d).	20
Figure 36S. ¹ H NMR (400 MHz, CD ₃ OD) of 3-(4-chlorophenyl)-4-morpholinobutanoic acid (9e).	21
Figure 37S. ¹³ C NMR (100 MHz, CD ₃ OD) of 3-(4-chlorophenyl)-4-morpholinobutanoic acid (9e).	21
Figure 38S. ¹ H NMR (400 MHz, CD ₃ OD) of 3-(4-chlorophenyl)-4-thiomorpholinobutanoic acid (9f).	22
Figure 39S. ¹³ C NMR (100 MHz, CD ₃ OD) of 3-(4-chlorophenyl)-4-thiomorpholinobutanoic acid (9f).	22
Figure 40S. 2D NMR (HETCOR 400 MHz, CD ₃ OD) of 3-(4-chlorophenyl)-4-thiomorpholinobutanoic acid (9f).	23

- Figure 41S.** Alignment of *pseudomonas fluorescens* (PF), human (HS), *E. coli* (EC) and wild boar (JB). Red and blue color letters corresponds to the residues of the chain A and chain B respectively, that interact with vigabatrin in the 1ohv crystal structure 24
- Figure 42S.** Validation of the molecular docking calculation for the pseudomonas model. Ligand in the PDB:ID 3r4t crystal structure was reproduced with a RMSD of 1.7 Å. Ligand experimental (opaque color) and calculated conformation (shiny color) are displayed as sticks representation respectively. Residues within 4.0 Å of both ligands are shown as thin sticks 25
- Figure 43S.** Validation of the molecular docking calculation for the human model. Ligand in the PDB:ID 1ohw crystal structure was reproduced with a RMSD of 1.3 Å. Ligand experimental (opaque color) and calculated conformation (shiny color) are displayed as sticks representation respectively. Residues within 4.0 Å of both ligands are shown as thin sticks. 25
- Figure 44S.** Validation of the molecular docking calculation for the human model. Ligand in the PDB:ID 1ohy crystal structure was reproduced with a RMSD of 1.8 Å. Ligand experimental (opaque color) and calculated conformation (shiny color) are displayed as sticks representation respectively. Residues within 4.0 Å of both ligands are shown as thin sticks. 26
- Figure 45S.** Optimized structures of all GABA analogues, VPNa and VGB. 27
- Figure 46S.** Interactions between GABA analogues 7 and *Pseudomonas fluorescens* GABA-AT. a) 7a, b) 7b, c) 7c, d) 7d, e) 7e and f) 7f. PLP prosthetic group is showed as Van der Waals spheres and each protein chain is colored in green and cyan. Residues at 4 Å of each analogue are indicated. Hydrogen bonds are shown as orange dashed lines. 30
- Figure 47S.** Interactions between GABA analogues 8 and *Pseudomonas fluorescens* GABA-AT. a) (S)-8a, b) (R)-8a, c) (S)-8b, d) (R)-8b, e) (S)-8c and f) (R)-8c, g) (S)-8d, h) (R)-8d, i) (S)-8e, j) (R)-8e, k) (S)-8f, l) (R)-8f. PLP prosthetic group is showed as Van der Waals spheres and each protein chain is colored in green and cyan. Residues at 4 Å of each analogue are indicated. Hydrogen bonds are shown as orange dashed lines. 31
- Figure 48S.** Interactions between GABA analogues 9 and *Pseudomonas fluorescens* GABA-AT. a) (S)-9c, b) (R)-9c, c) (S)-9d and d) (R)-9d, e) (S)-9e, f) (R)-9e, g) (S)-9f, h) (R)-9f. PLP prosthetic group is showed as Van der Waals spheres and each protein chain is colored in green and cyan. Residues at 4 Å of each analogue are indicated. Hydrogen bonds are shown as orange dashed lines. 33

Table 1S. Energy interactions values obtained from the docking calculations of all GABA derivatives and *pseudomonas* GABA-AT model. All the values are in kcal/mol. 34

Figure 49S. Interactions between GABA analogues 7 and *Human* GABA-AT. a) 7a, b) 7b, c) 7c, d) 7d, e) 7e and f) 7f. PLP prosthetic group is showed as Van der Waals spheres and each protein chain is colored in yellow and red. Residues at 4 Å of each analogue are indicated. Hydrogen bonds are shown as orange dashed lines. 35

Figure 50S. Interactions between GABA analogues 8 and *Human* GABA-AT. a) (S)-8a, b) (R)-8a, c) (S)-8b, d) (R)-8b, e) (S)-8c and f) (R)-8c, g) (S)-8d, h) (R)-8d, i) (S)-8e, j) (R)-8e, k) (S)-8f, l) (R)-8f. PLP prosthetic group is showed as Van der Waals spheres and each protein chain is colored in yellow and red. Residues at 4 Å of each analogue are indicated. Hydrogen bonds are shown as orange dashed lines. 37

Figure 51S. Interactions between GABA analogues 9 and *Human* GABA-AT. a) (S)-9b, b) (R)-9b, c) (S)-9c and d) (R)-9c, e) (S)-9d, f) (R)-9d, g) (S)-9e, h) (R)-9e, i) (S)-9f, j) (R)-9f. PLP prosthetic group is showed as Van der Waals spheres and each protein chain is colored in yellow and red. Residues at 4 Å of each analogue are indicated. Hydrogen bonds are shown as orange dashed lines. 39

Figure 52S. Backbone structural alignment of GABA-AT structures. a) GABA-AT human model in cyan color. 1ohv, 1ohw and 1ohy *Sus scrofa* crystal structures in red (RMSD=0.35), gray (RMSD=0.36) and orange (RMSD=0.40) color respectively. b) GABA-AT *Pseudomonas fluorescens* model in shiny red color, 1sf2 *E. coli* structure in shiny yellow color (RMSD= 0.52). Fe₂S₂ (yellow/pink color) and PLP from human model in VDW representation. 40

Table 2S. Energy interactions values obtained from the docking calculations of all GABA derivatives and *human* GABA-AT model. All the values are in kcal/mol. 41

Table 3S. Values of the experimental (Y_{Exp}), calculated (Y_{Cal}) and predicted (Y_{Pred}) percent of inhibition of the GABA derivatives. Compounds that were considered form the test validation are marked with a script symbol. 42

NMR Spectra of compounds.

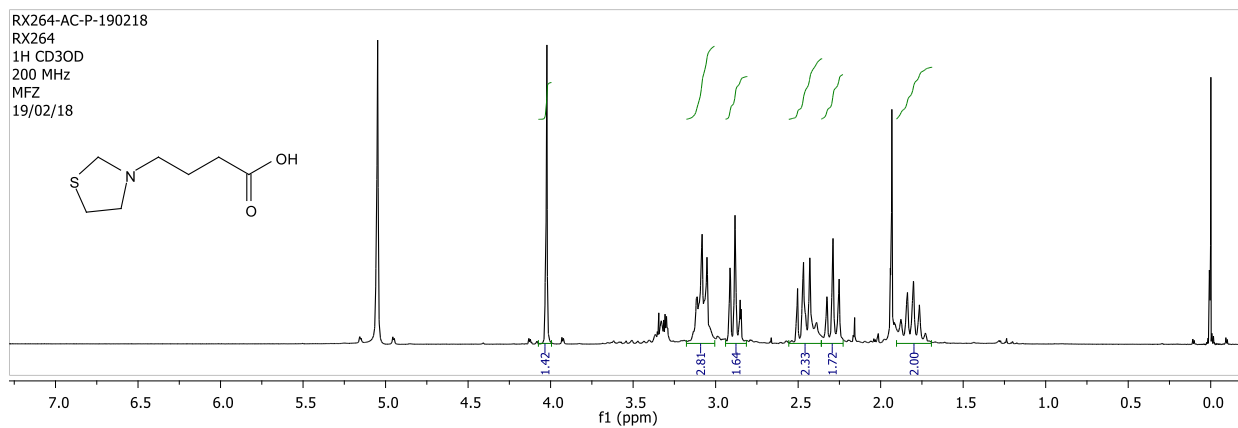


Figure 1S. ^1H NMR (200 MHz, CD_3OD) of 4-(thiazolidin-3-yl)butanoic acid (**7a**).

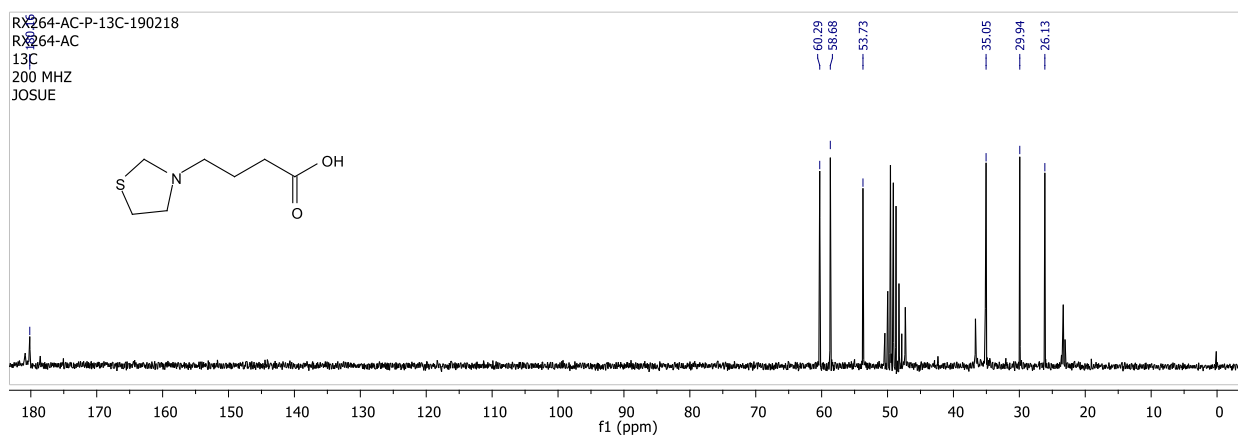


Figure 2S. ^{13}C NMR (50 MHz, CD_3OD) of 4-(thiazolidin-3-yl)butanoic acid (**7a**)

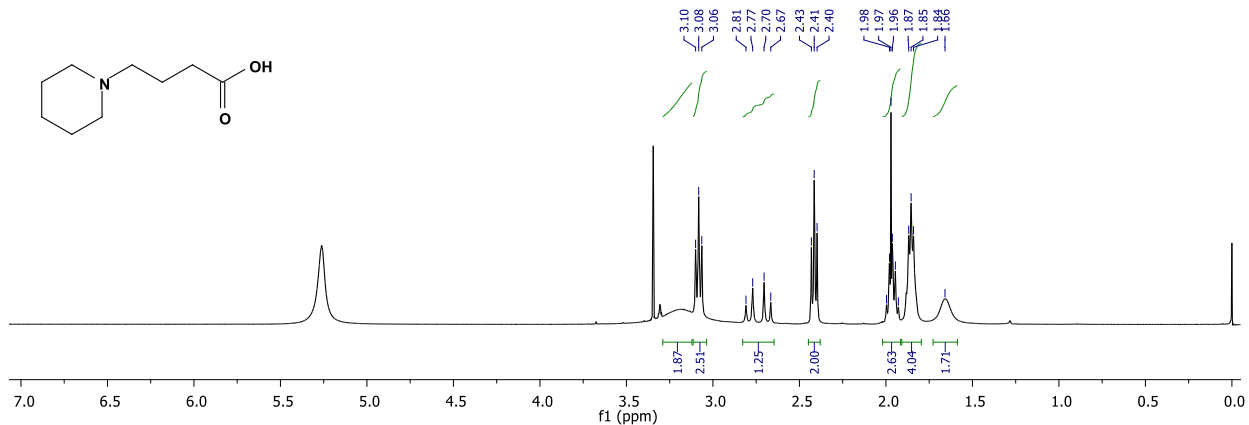


Figure 3S. ^1H NMR (400 MHz, CD_3OD) of 4-(piperidin-1-yl)butanoic acid (**7b**).

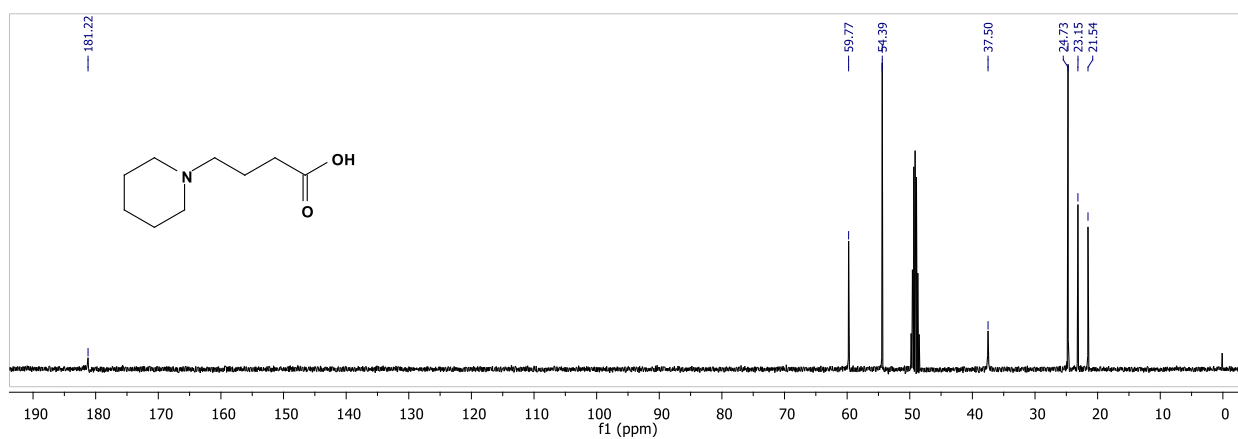


Figure 4S. ^{13}C NMR (400 MHz, CD_3OD) of 4-(piperidin-1-yl)butanoic acid (**7b**).

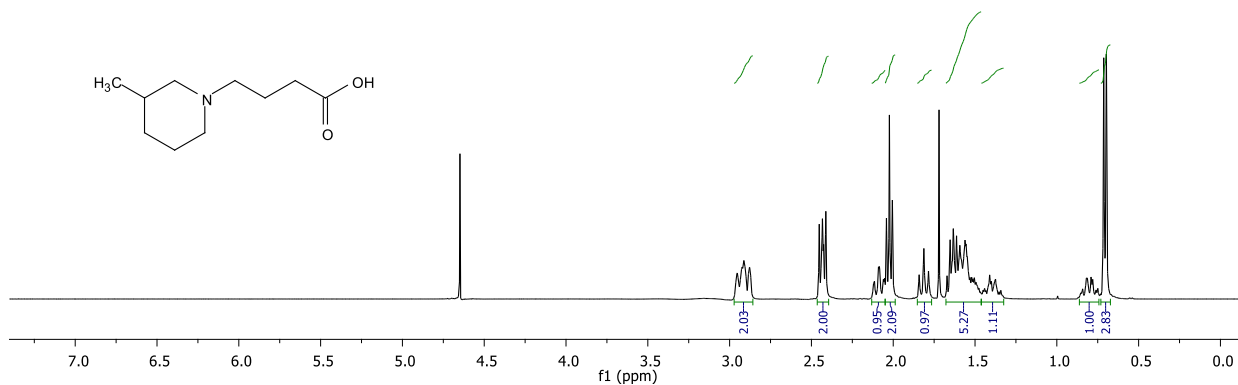


Figure 5S. ^1H NMR (400 MHz, D_2O) of 4-(3-methylpiperidin-1-yl)butanoic acid (**7c**).

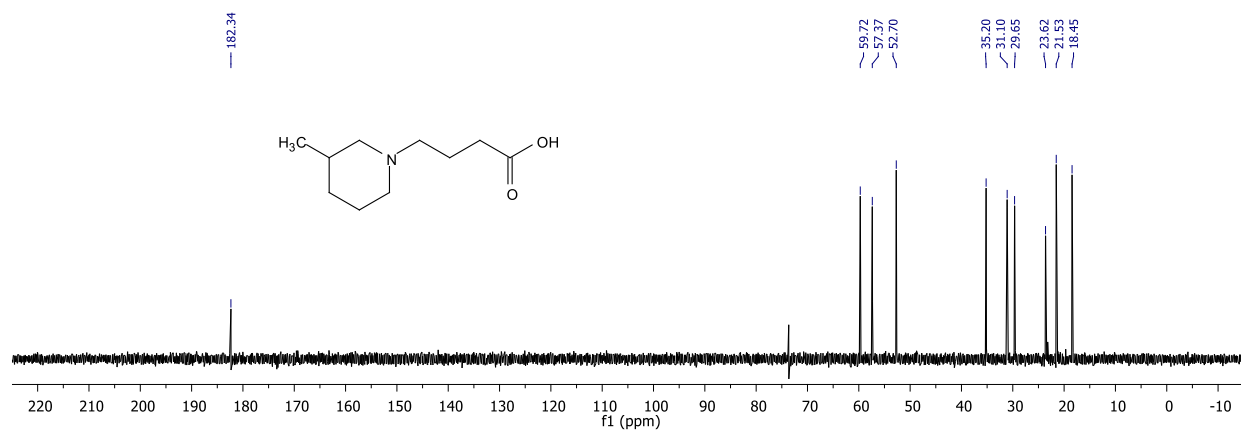


Figure 6S. ¹³C NMR (100 MHz, D₂O) of sodium 4-(3-methylpiperidin-1-yl)butanoic acid (7c).

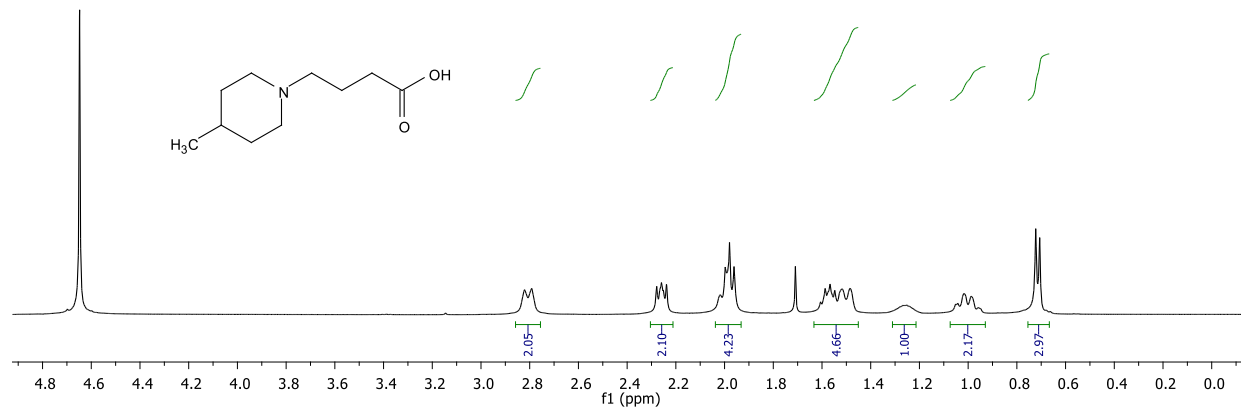


Figure 7S. ¹H NMR (400 MHz, CD₃OD) of 4-(4-methylpiperidin-1-yl)butanoic acid (7d).

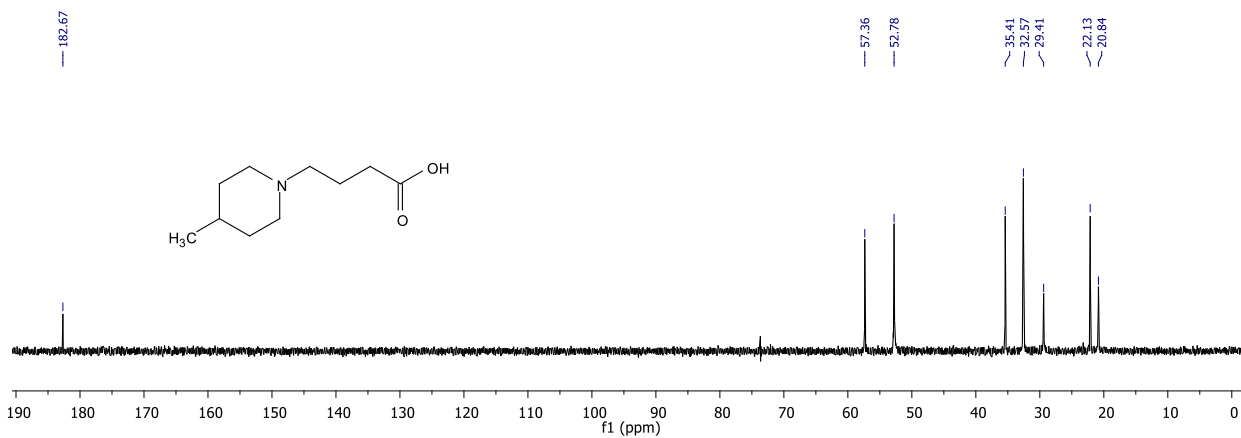


Figure 8S. ¹³C NMR (100 MHz, CD₃OD) of 4-(4-methylpiperidin-1-yl)butanoic acid (7d).

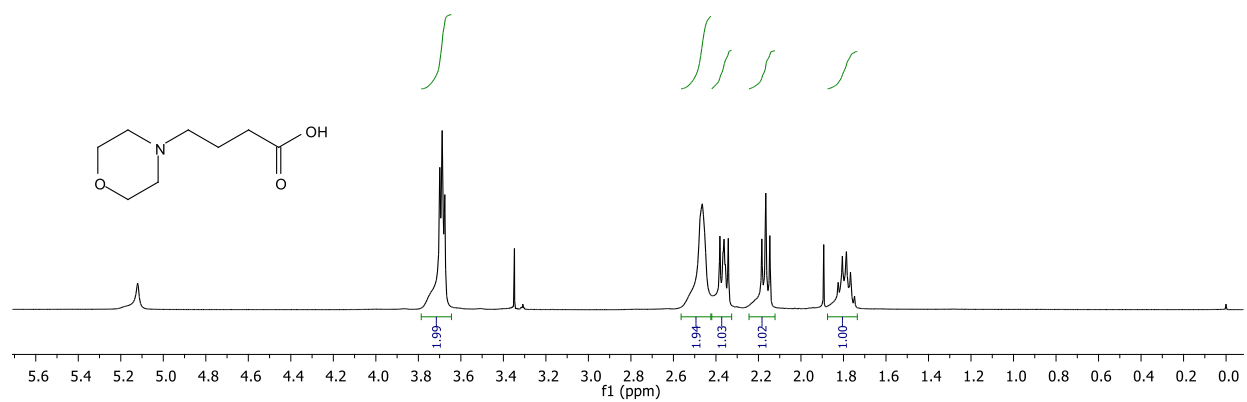


Figure 9S. ¹H NMR (400 MHz, CD₃OD) of 4-morpholinobutanoic acid (7e).

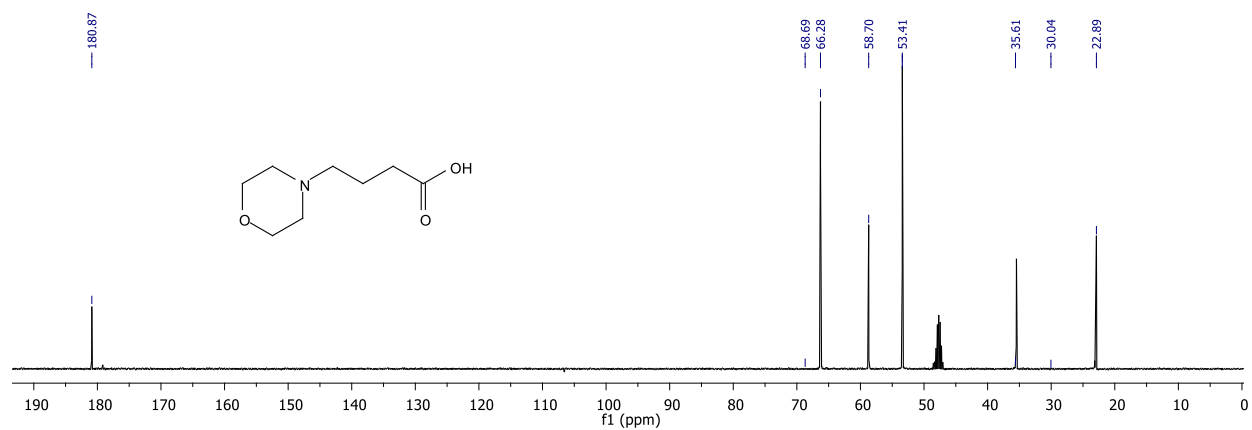


Figure 10S. ¹³C NMR (100 MHz, CD₃OD) of 4-morpholinobutanoic acid (7e).

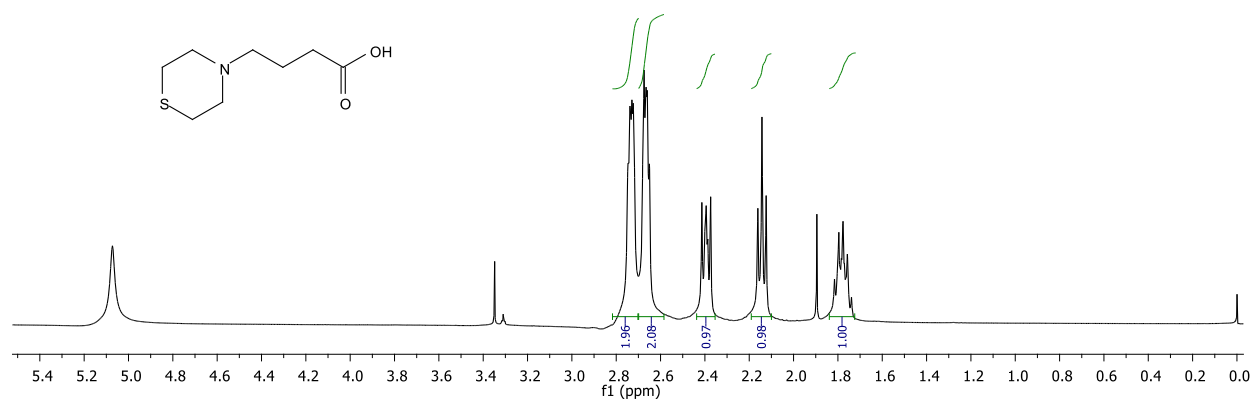


Figure 11S. ¹H NMR (400 MHz, CD₃OD) of 4-thiomorpholinobutanoic acid (7f).

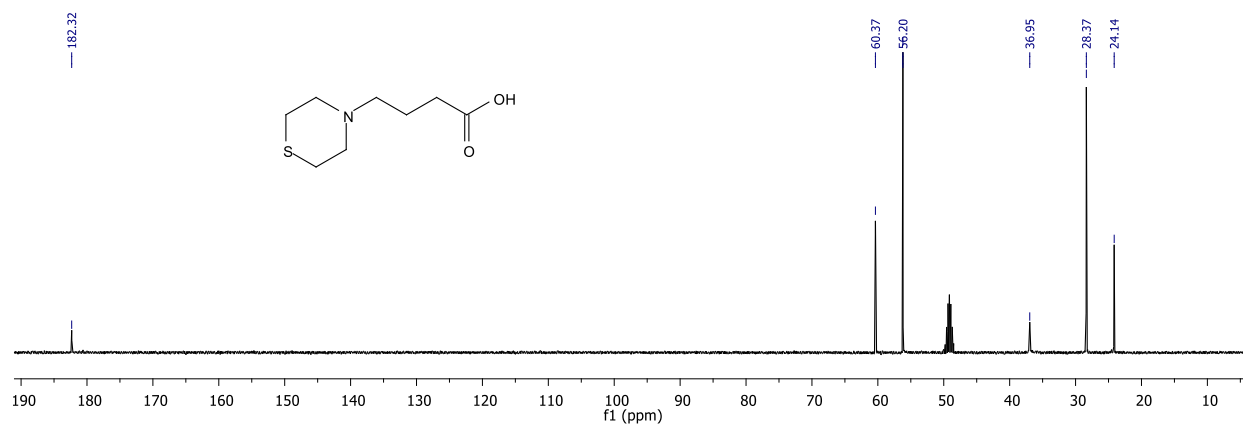


Figure 12S. ^{13}C NMR (100 MHz, CD_3OD) of 4-thiomorpholinobutanoic acid (7f).

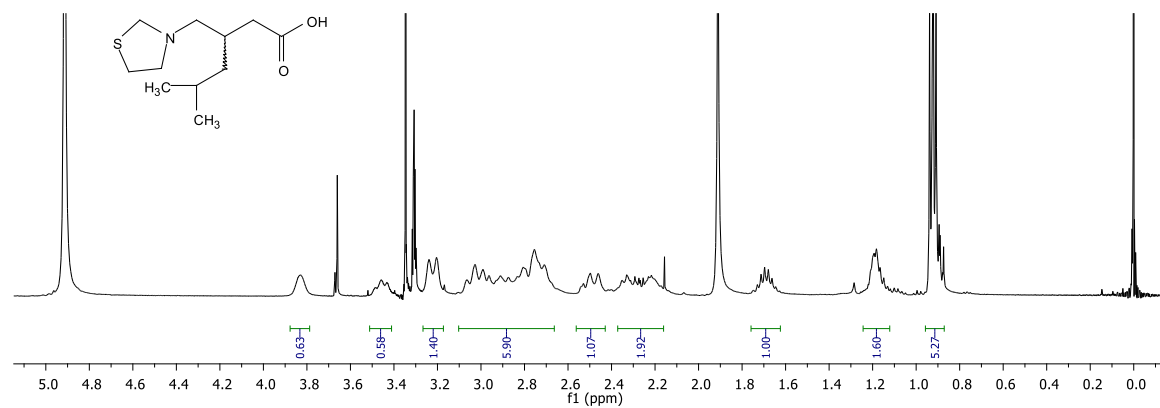


Figure 13S. ^1H NMR (400 MHz, CD_3OD) of 5-methyl-3-(thiazolidin-3-ylmethyl)hexanoic acid (8a).

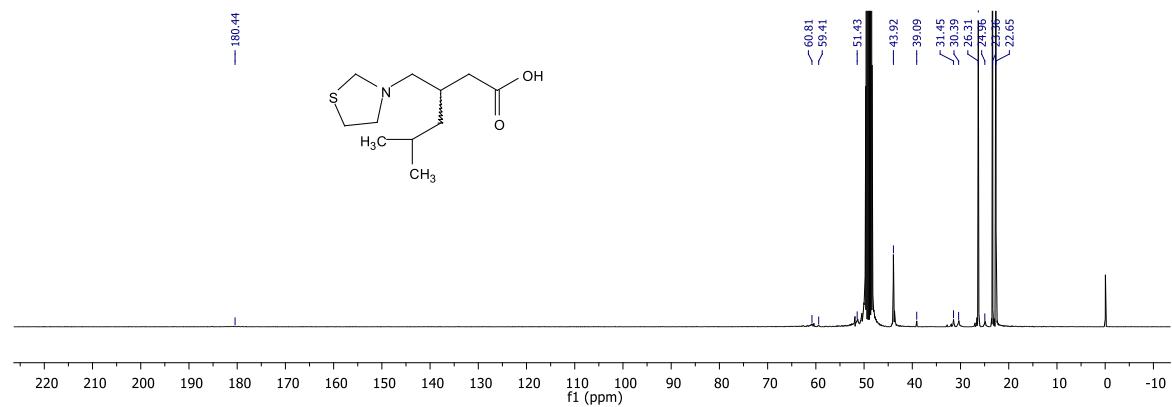


Figure 14S. ^{13}C NMR (100 MHz, CD_3OD) of 5-methyl-3-(thiazolidin-3-ylmethyl)hexanoic acid (8a).

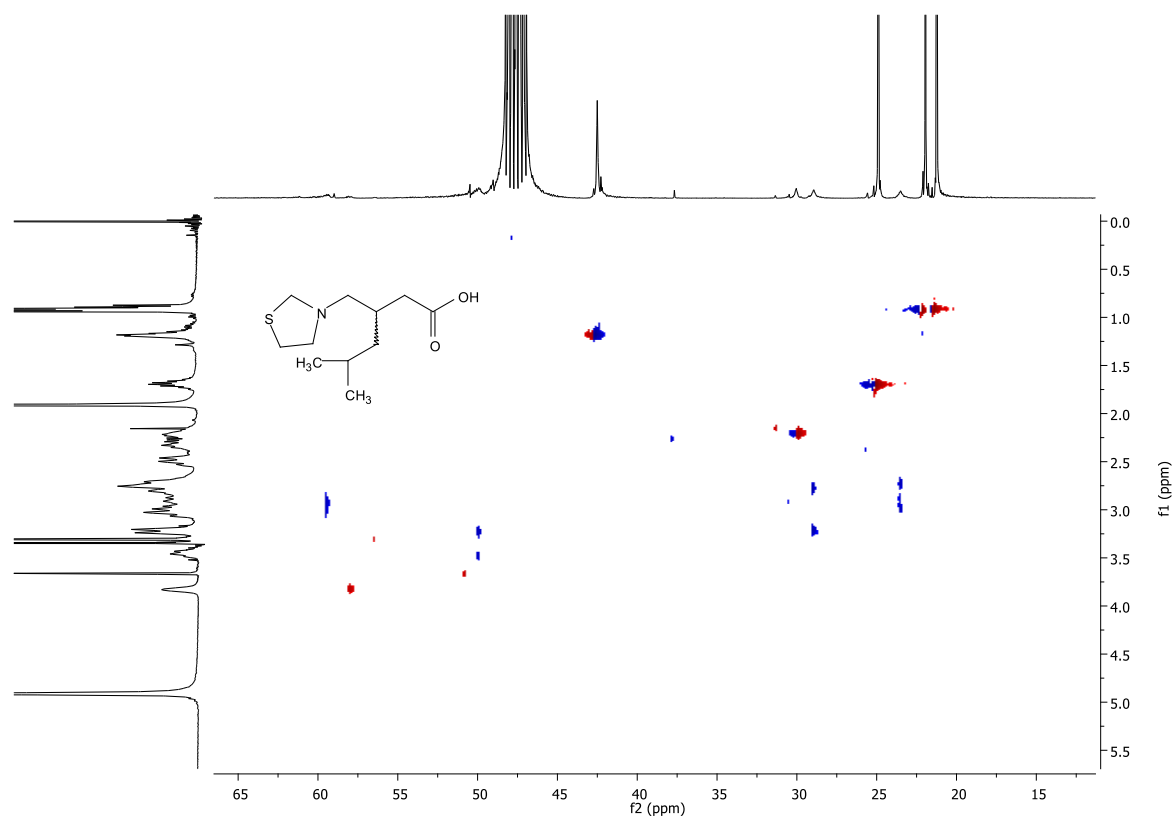


Figure 15S. 2D NMR (HETCOR 400 MHz, CD₃OD) of 5-methyl-3-(thiazolidin-3-ylmethyl)hexanoic acid (**8a**).

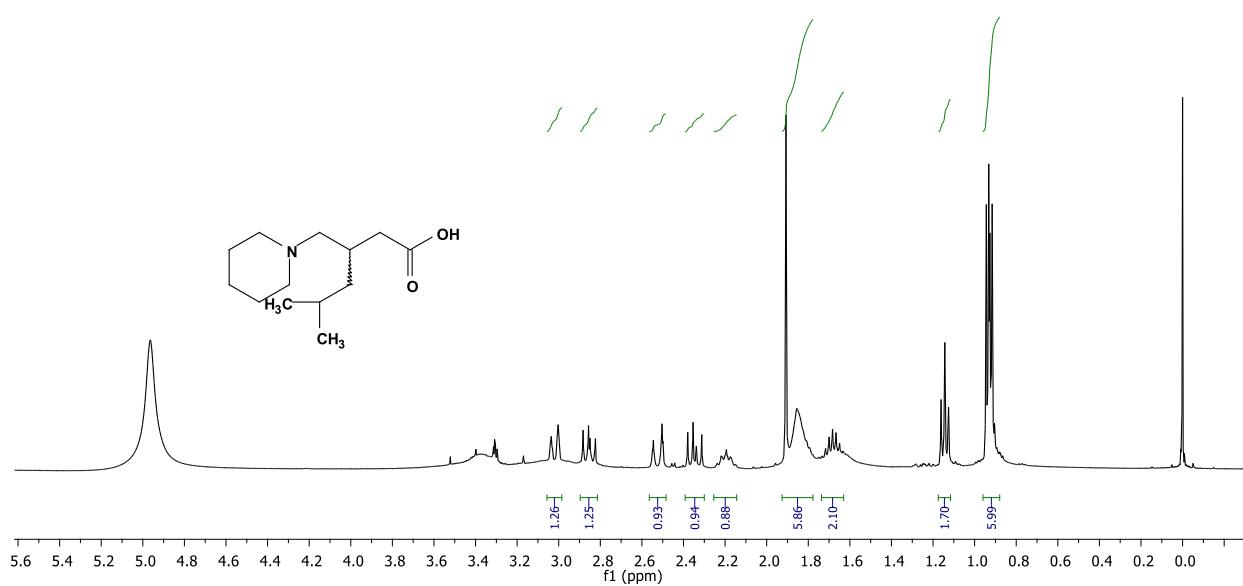


Figure 16S. ¹H NMR (400 MHz, CD₃OD) of 5-methyl-3-(piperidin-1-ylmethyl)hexanoic acid (**8b**).

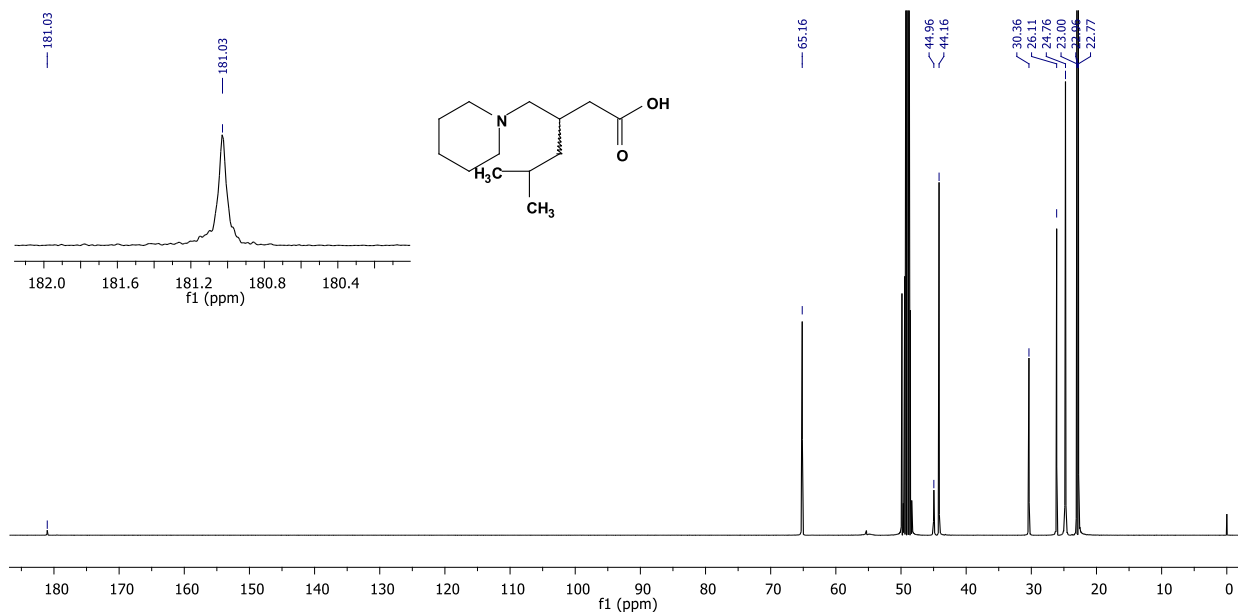


Figure 17S. ¹³C NMR (100 MHz, CD₃OD) of 5-methyl-3-(piperidin-1-ylmethyl)hexanoic acid (**8b**).

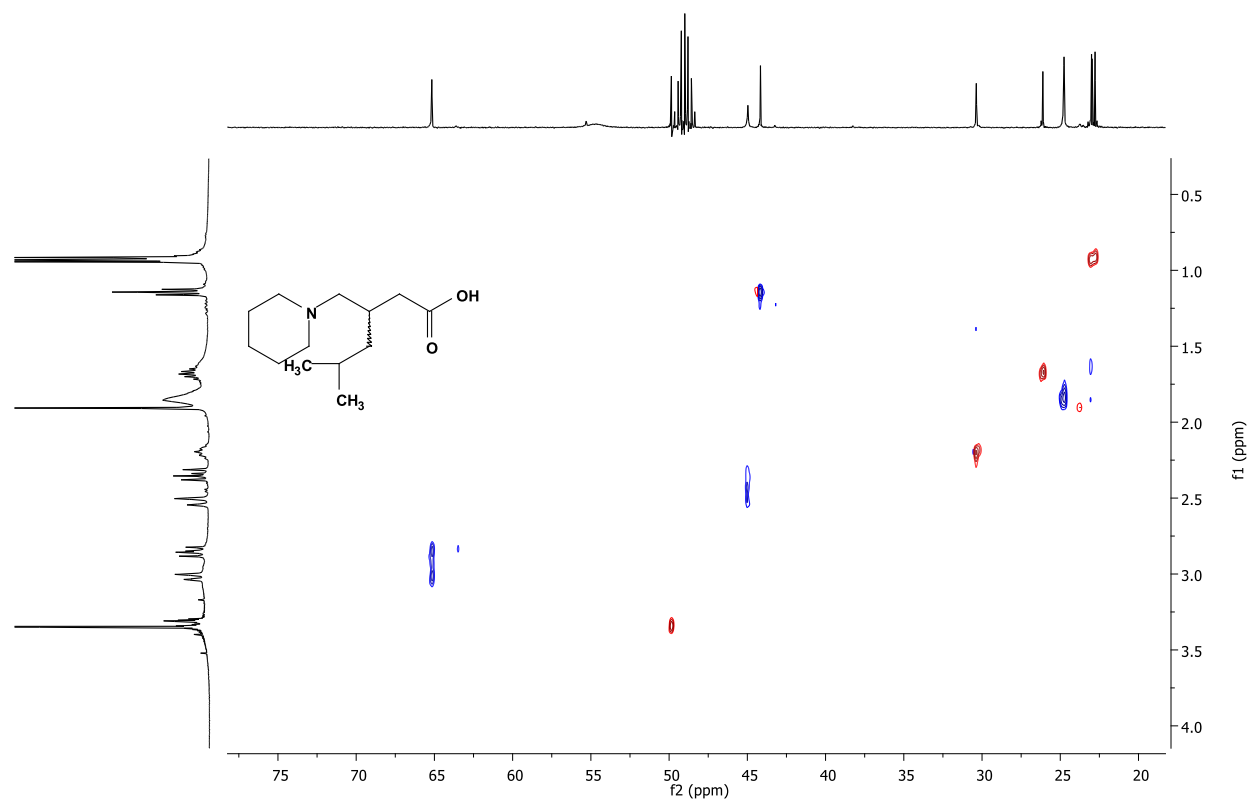


Figure 18S. 2D NMR (HETCOR 400 MHz, CD₃OD) of 5-methyl-3-(piperidin-1-ylmethyl) hexanoic acid (**8b**).

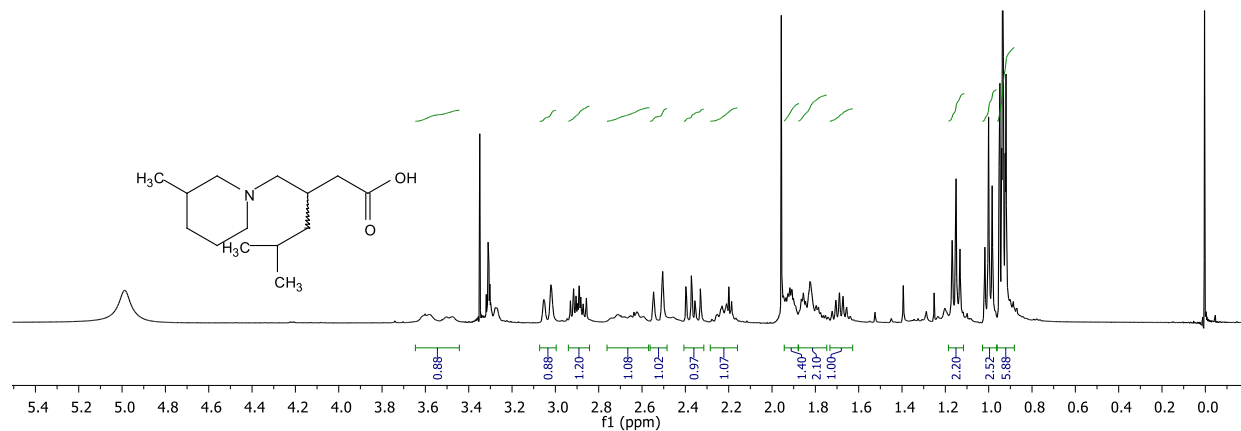


Figure 19S. ^1H NMR (400 MHz, CD_3OD) of 5-methyl-3-((3-methylpiperidin-1-yl)methyl)hexanoic acid (8c).

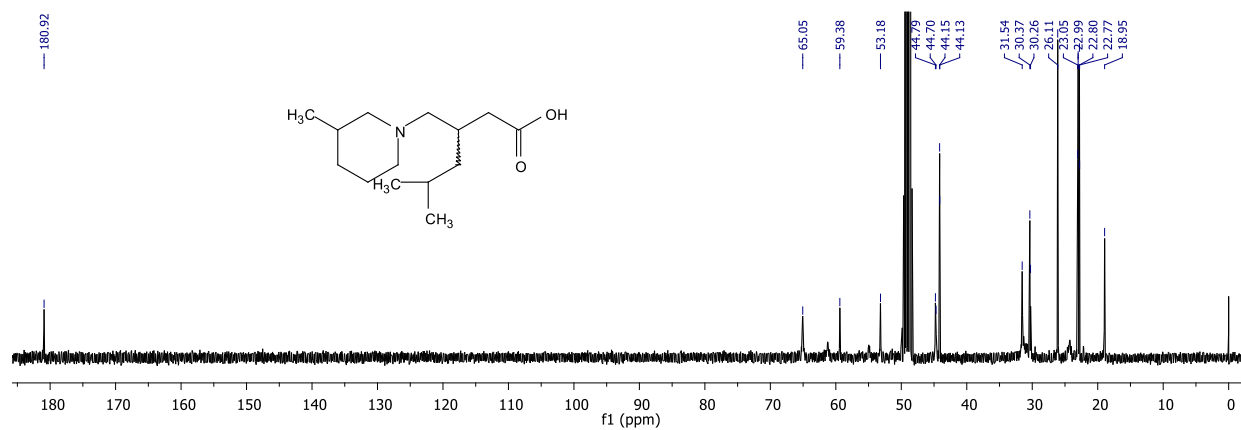


Figure 20S. ^{13}C NMR (100 MHz, CD_3OD) of 5-methyl-3-((3-methylpiperidin-1-yl)methyl)hexanoic acid (8c).

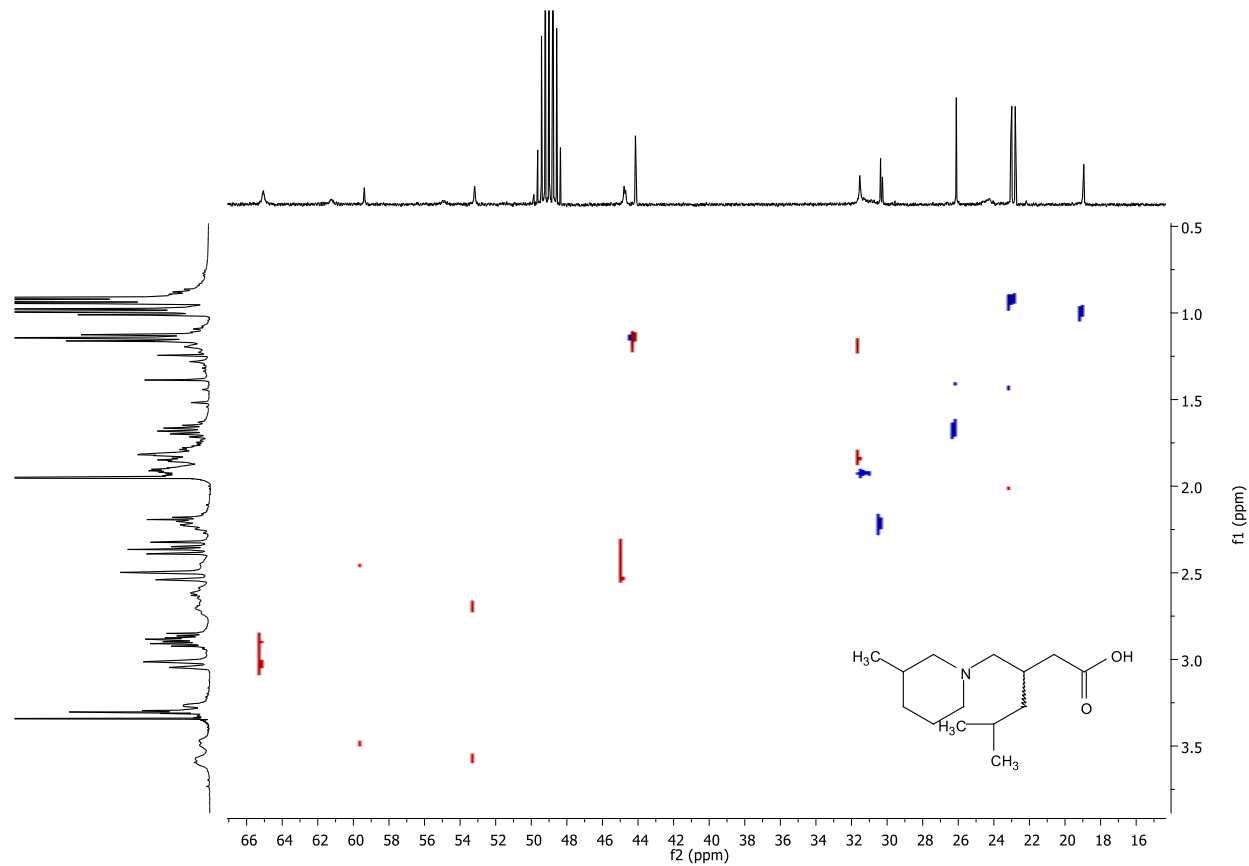


Figure 21S. 2D NMR (HETCOR 400 MHz, CD₃OD) of 5-methyl-3-((3-methylpiperidin-1-yl)methyl)hexanoic acid (**8c**).

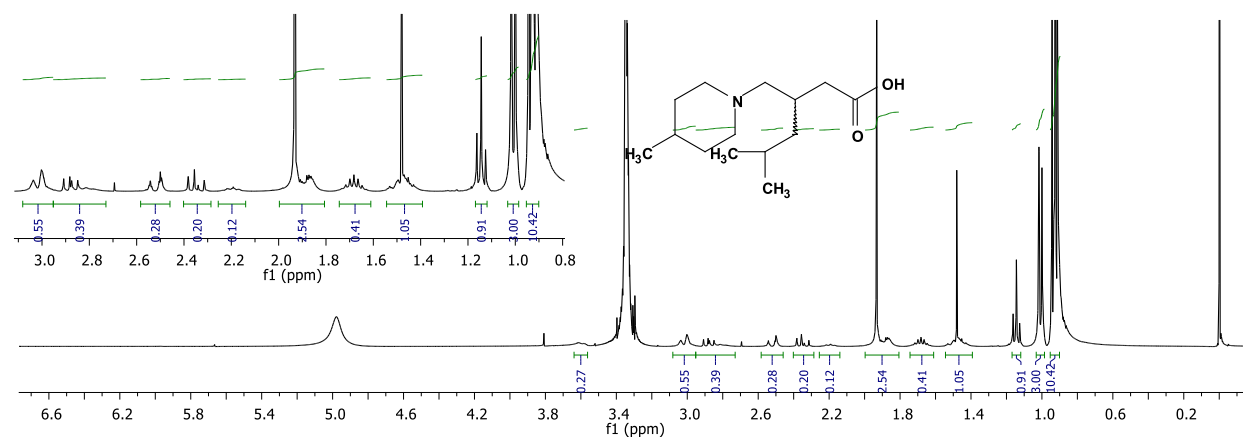


Figure 22S. ¹H NMR (400 MHz, CD₃OD) of 5-methyl-3-((4-methylpiperidin-1-yl)methyl)hexanoic acid (**8d**).

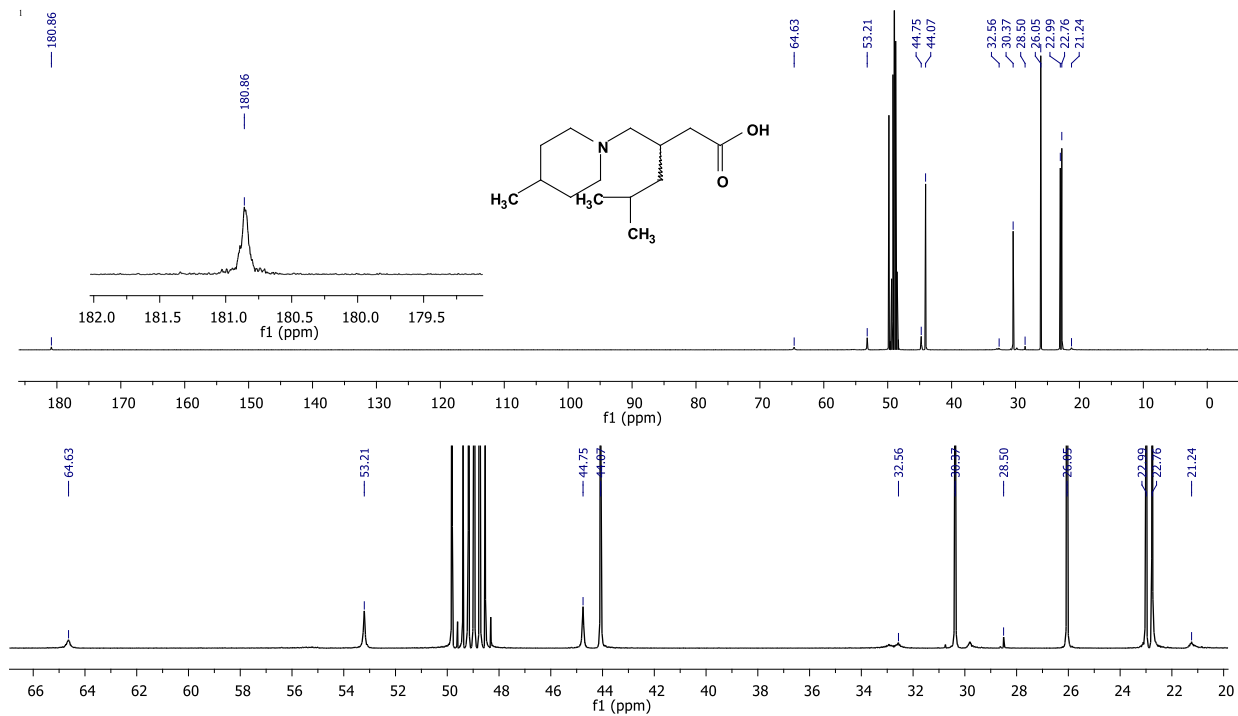


Figure 23S. ¹³C NMR (100 MHz, CD₃OD) of 5-methyl-3-((4-methylpiperidin-1-yl)methyl)hexanoic acid (8d).

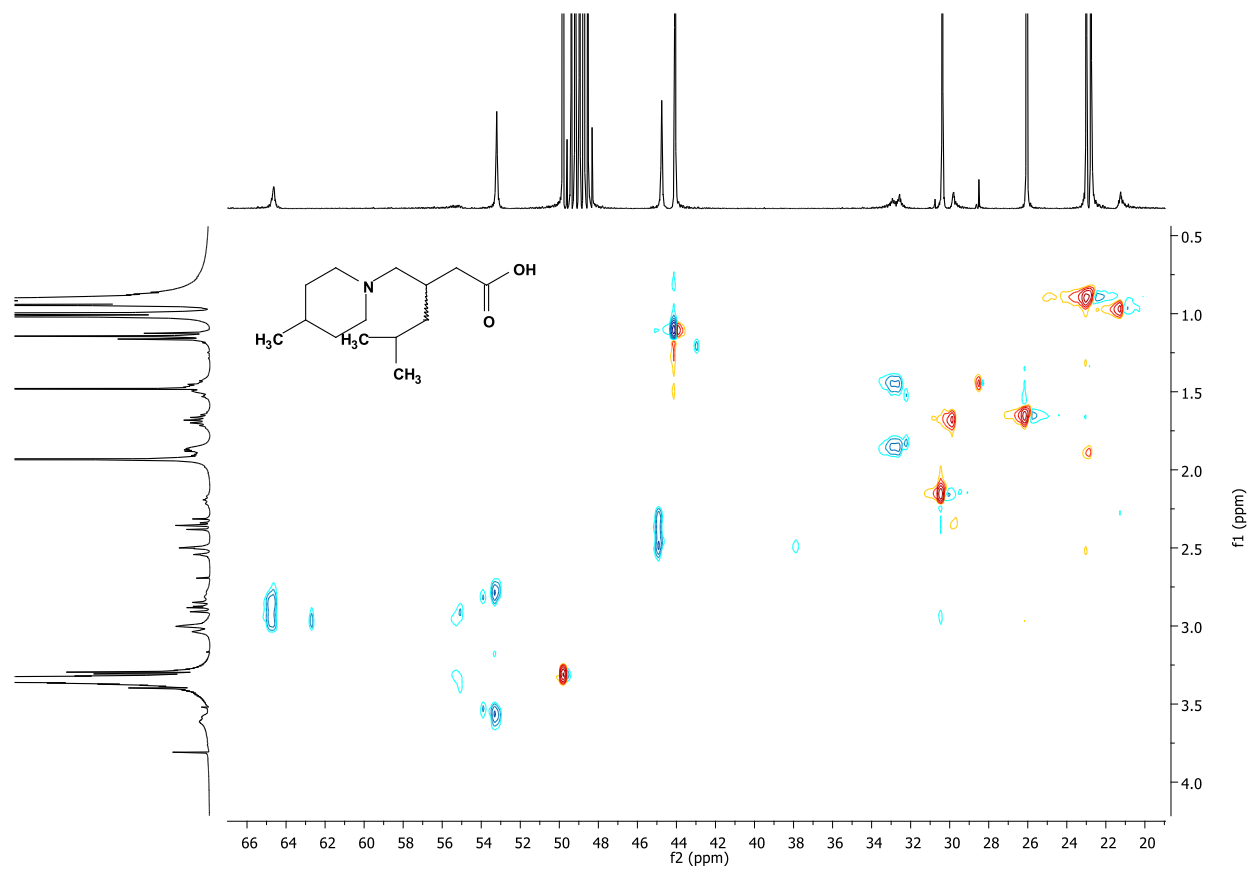


Figure 24S. 2D NMR (HETCOR 400 MHz, CD_3OD) of 5-methyl-3-((4-methylpiperidin-1-yl)methyl)hexanoic acid (**8d**).

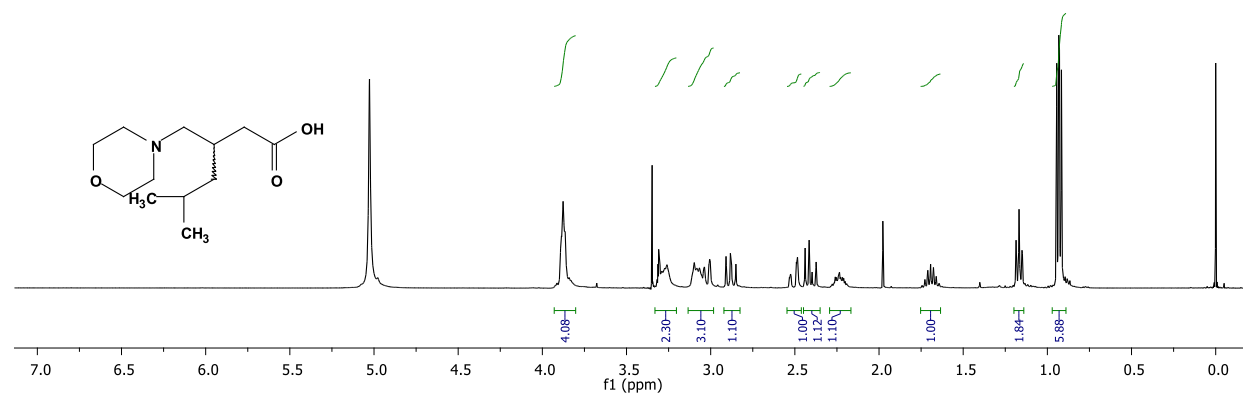


Figure 25S. ^1H NMR (400 MHz, CD_3OD) of 5-methyl-3-(morpholinomethyl) hexanoic acid (**8e**).

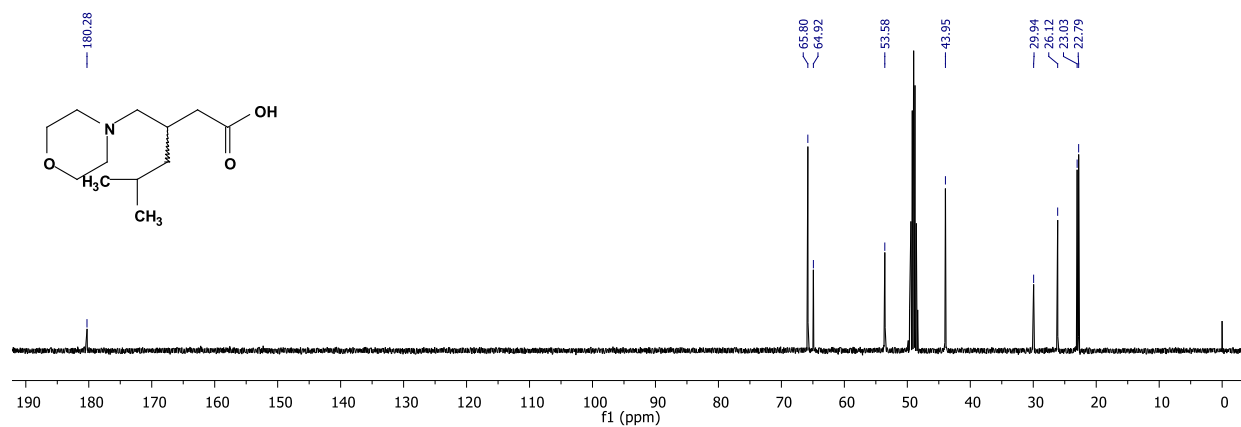


Figure 26S. ¹³C NMR (100 MHz, CD₃OD) of 5-methyl-3-(morpholinomethyl)hexanoic acid (8e).

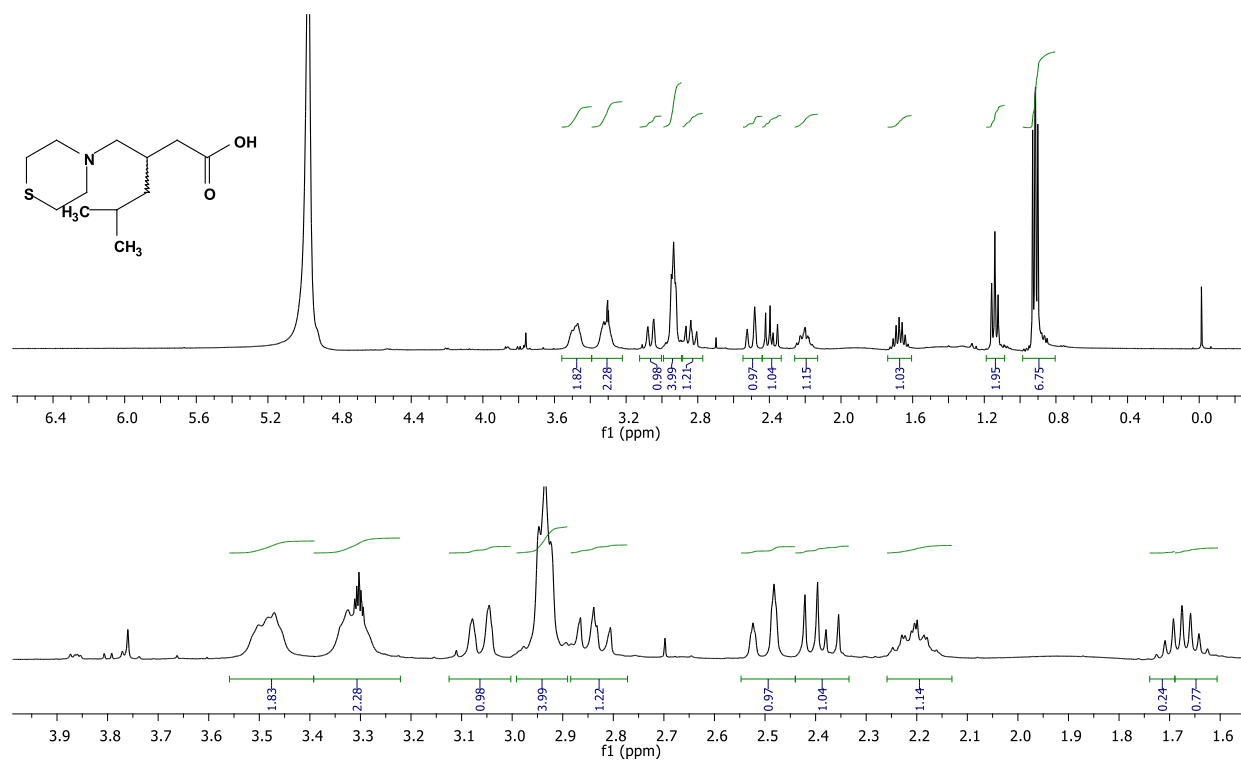


Figure 27S. ¹H NMR (400 MHz, CD₃OD) of 5-methyl-3-(thiomorpholinomethyl)hexanoic acid (8e).

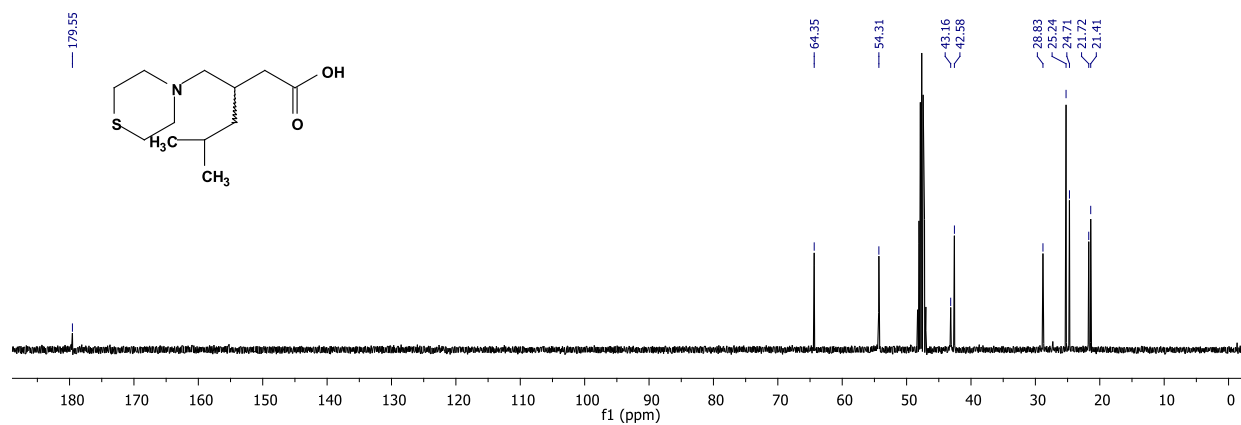


Figure 28S. ¹³C NMR (100 MHz, CD₃OD) of 5-methyl-3-(thiomorpholinomethyl)hexanoic acid (8f).

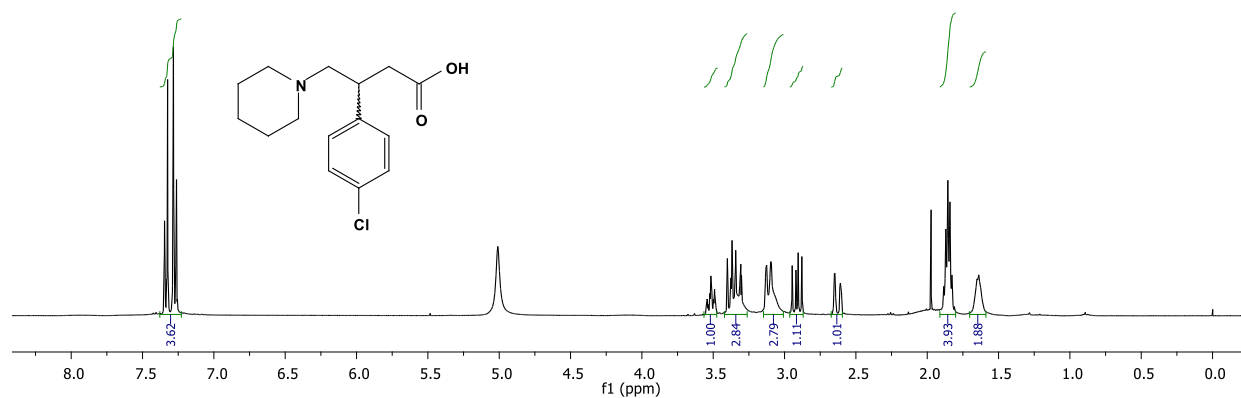


Figure 29S. ¹H NMR (400 MHz, CD₃OD) of 3-(4-chlorophenyl)-4-(piperidin-1-yl)butanoic acid (9b).

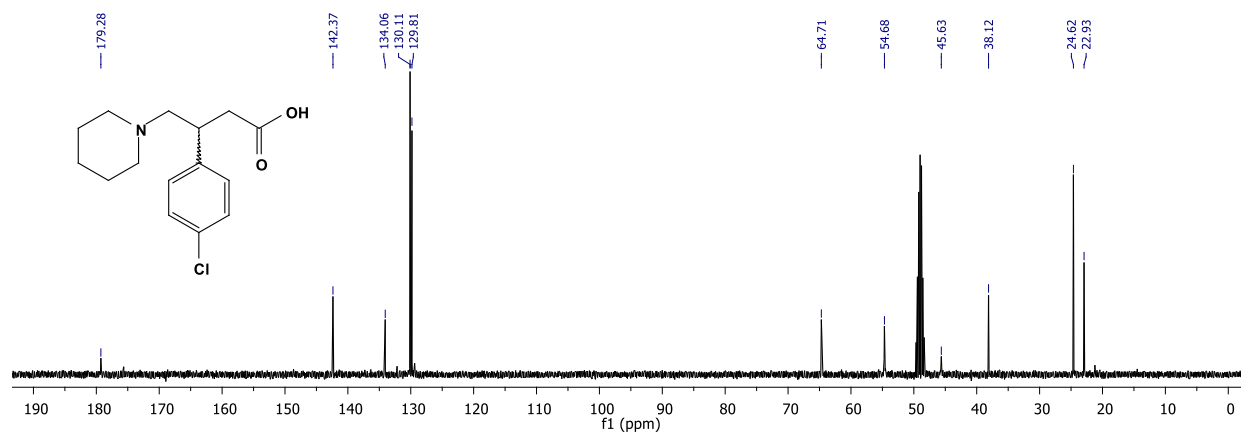


Figure 30S. ¹³C NMR (100 MHz, CD₃OD) of 3-(4-chlorophenyl)-4-(piperidin-1-yl)butanoic acid (9b).

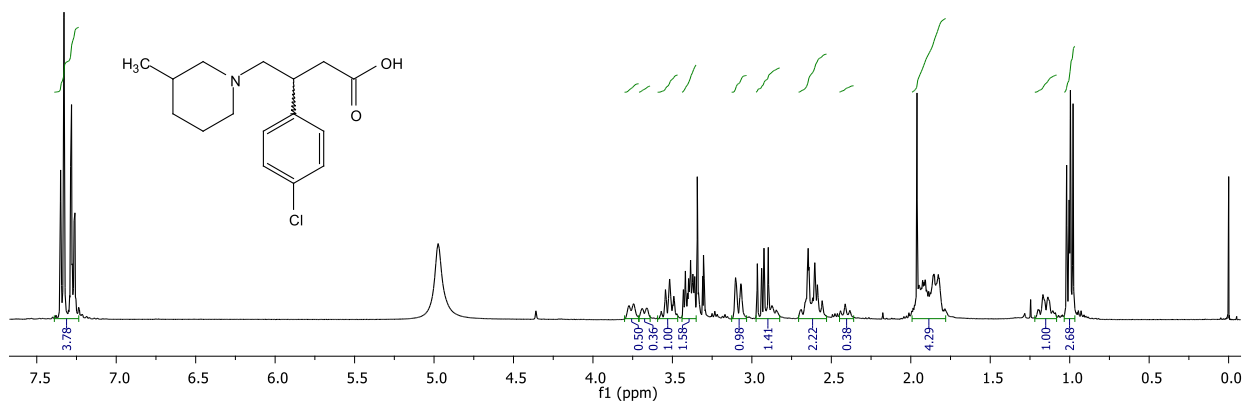


Figure 31S. ¹H NMR (400 MHz, CD₃OD) of 3-(4-chlorophenyl)-4-(3-methylpiperidin-1-yl)butanoic acid (9c).

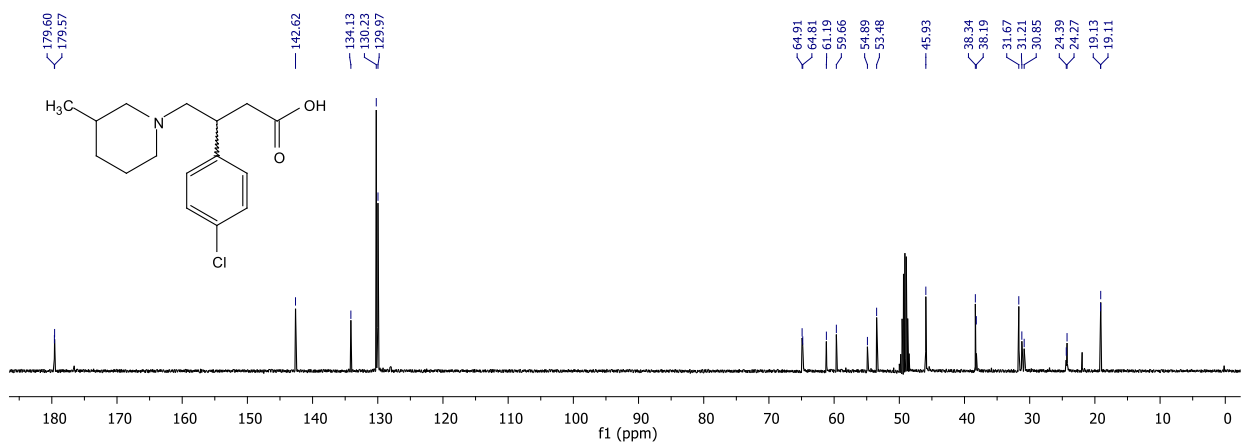


Figure 32S. ¹³C NMR (100 MHz, CD₃OD) of 3-(4-chlorophenyl)-4-(3-methylpiperidin-1-yl)butanoic acid (9c).

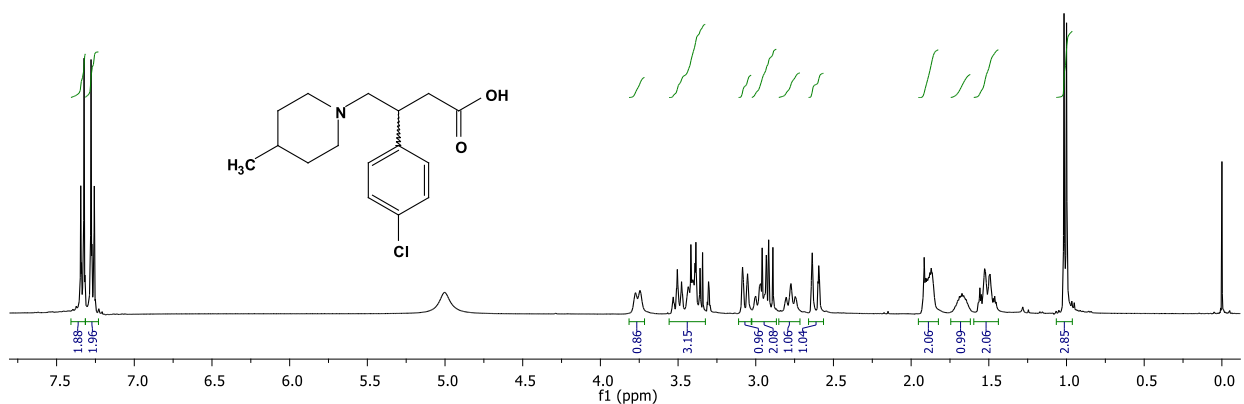


Figure 33S. ¹H NMR (400 MHz, CD₃OD) of 3-(4-chlorophenyl)-4-(4-methylpiperidin-1-yl)butanoic acid (9d).

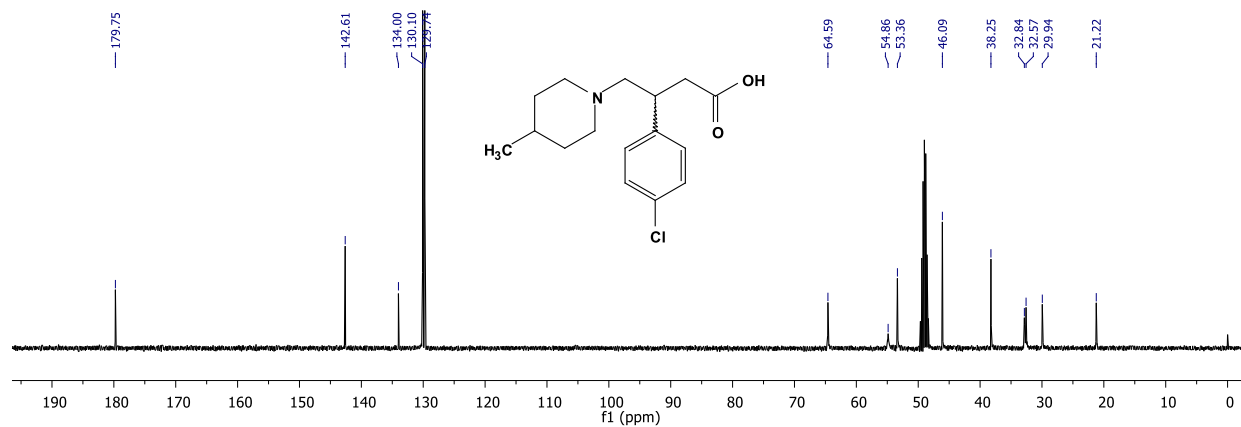


Figure 34S. ¹³C NMR (100 MHz, CD₃OD) of 3-(4-chlorophenyl)-4-(4-methylpiperidin-1-yl)butanoic acid (9d).

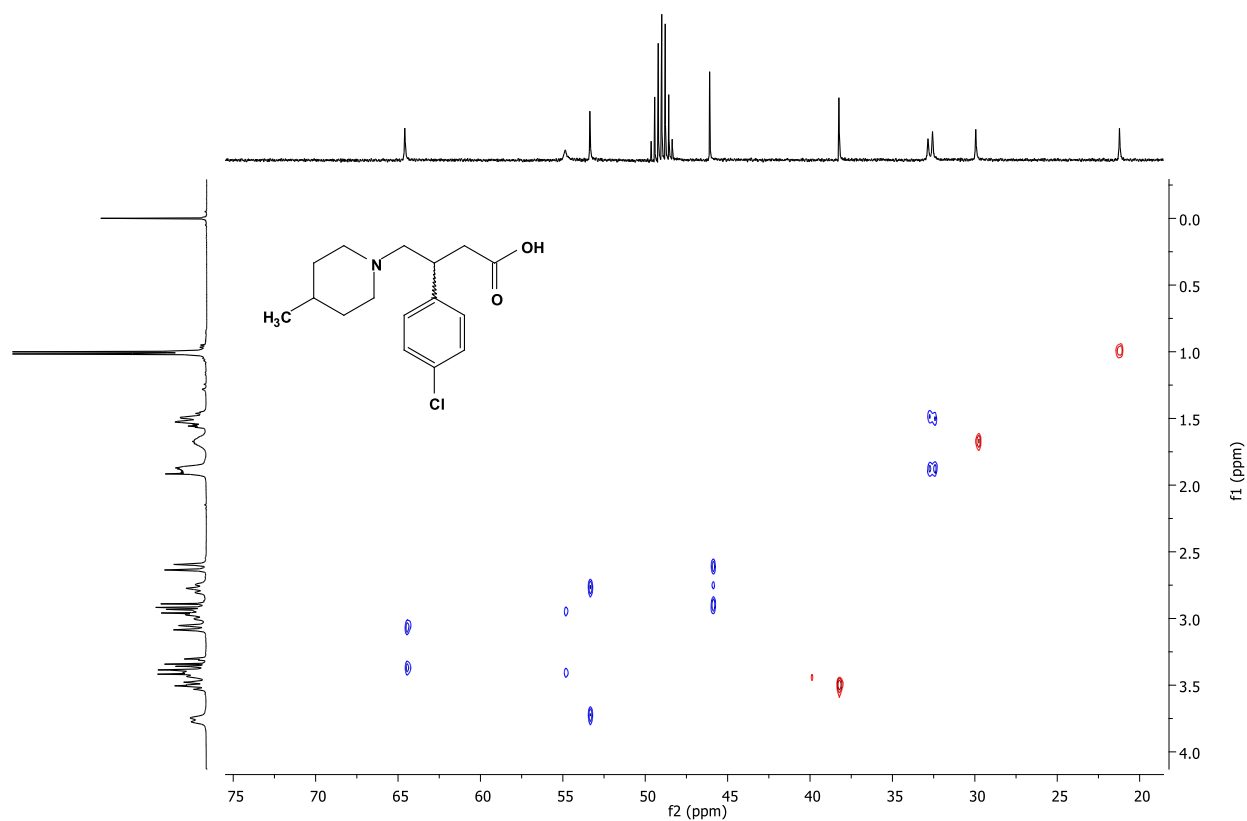


Figure 35S. 2D NMR (HETCOR 400 MHz, CD₃OD) of 3-(4-chlorophenyl)-4-(4-methylpiperidin-1-yl)butanoic acid (9d).

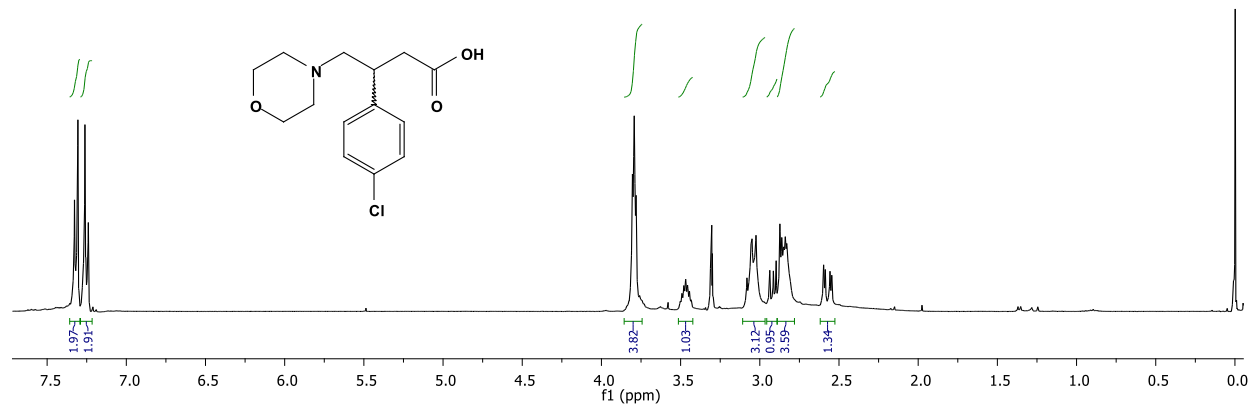


Figure 36S. ¹H NMR (400 MHz, CD₃OD) of 3-(4-chlorophenyl)-4-morpholinobutanoic acid (9e).

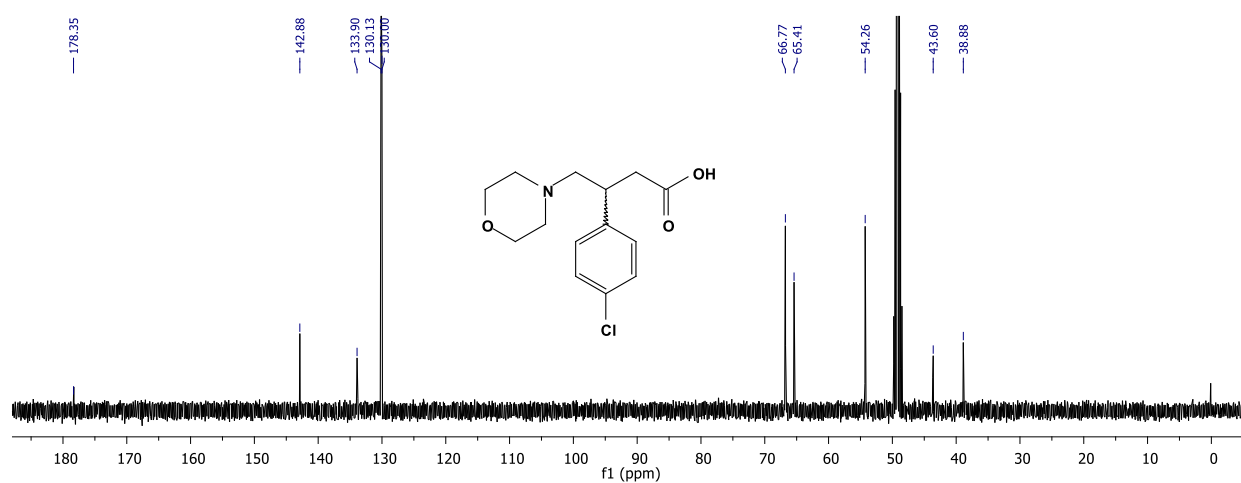
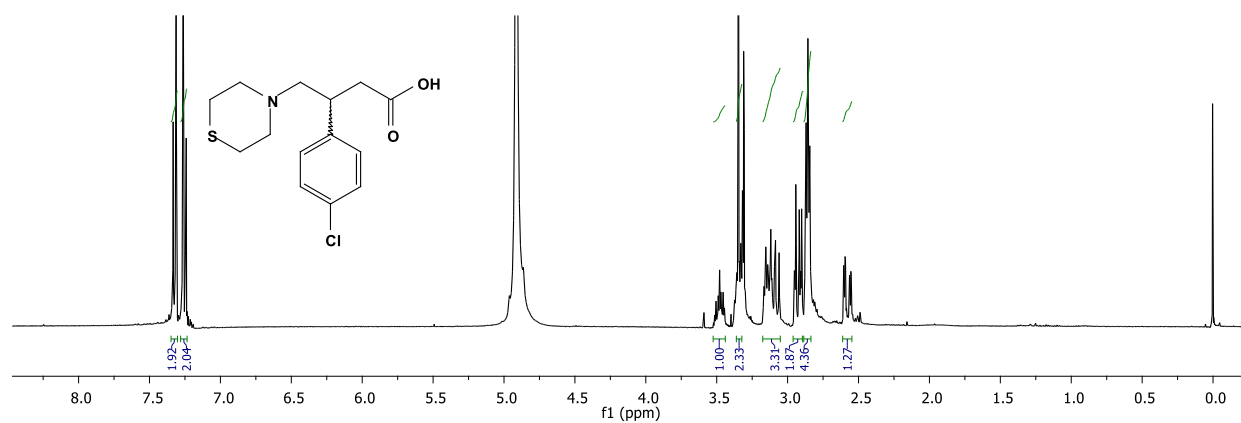


Figure 37S. ¹³C NMR (100 MHz, CD₃OD) of 3-(4-chlorophenyl)-4-morpholinobutanoic acid (9e).



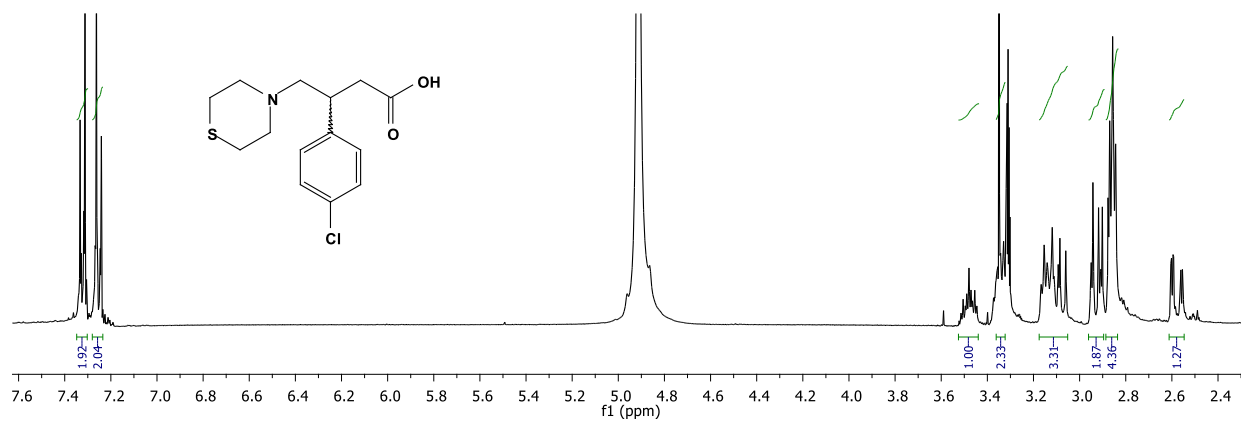


Figure 38S. ¹H NMR (400 MHz, CD₃OD) of 3-(4-chlorophenyl)-4-thiomorpholinobutanoic acid (9f).

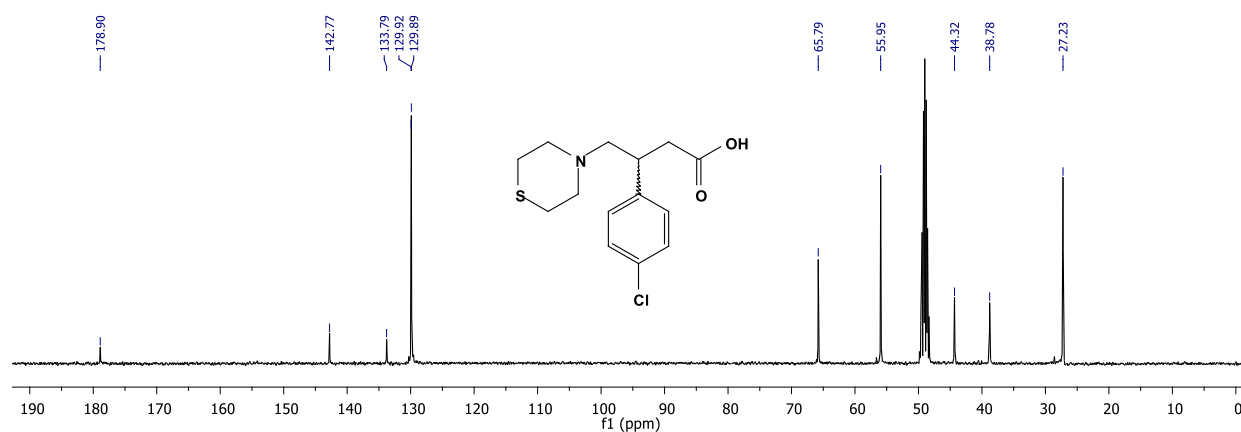


Figure 39S. ¹³C NMR (100 MHz, CD₃OD) of 3-(4-chlorophenyl)-4-thiomorpholinobutanoic acid (9f).

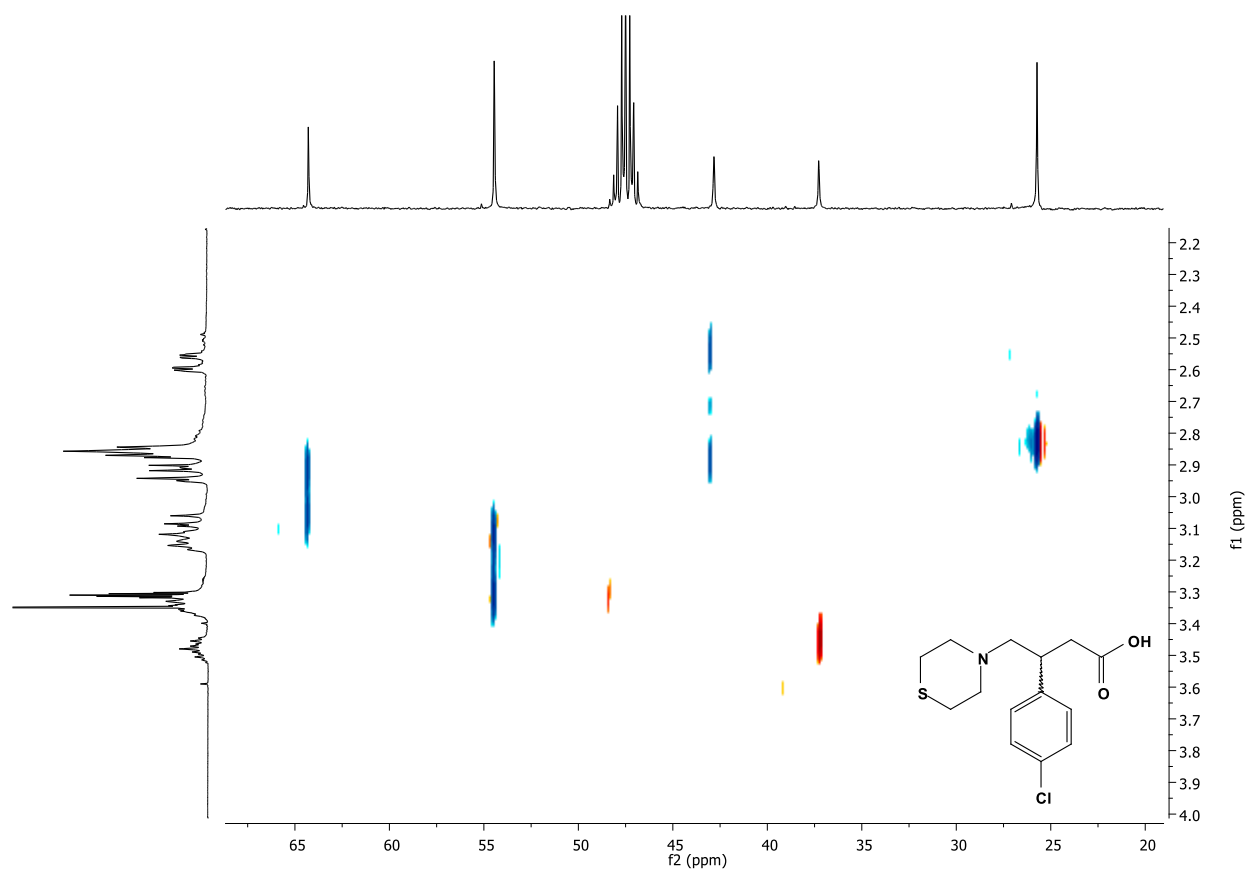


Figure 40S. 2D NMR (HETCOR 400 MHz, CD₃OD) of 3-(4-chlorophenyl)-4-thiomorpholinobutanoic acid (9f).

Computational Details

```
PF -----MSNKTNASLMKRREAAVPRGVGQIHP-IFAESAKNATVTDVEGREFID
EC -----NSNKELMQRRSQAI PRGVGQIHPI-FADRAENCRVWDVEGREYLD
HS -FDYDGPLMKTEVPGPRSQELMKQLNII--QNAEAVHFFCNYEESRGNYLVDVDGNRMLD
JB -FDYDGPLMKTEVPGPRSRELMKQLNII--QNAEAVHFFCNYEESRGNYLVDVDGNRMLD

PF FAGGIAAVLNTGHLHPKIIAAVTEQLNKLTH---TCFQVLAYEPYVELCEKVNAK-VPGDF
EC FAGGIAAVLNTGHLHPKVVA AVEAQLKKLSH---TCFQVLAYEPYLELCEI-MNQKVPGDF
HS LYSQISSVPIGYSHPALLKLIQQPQNASMFVNRPALGILPPENFVEKLRQSLLSVAPKGM
JB LYSQISSIPIGYSHPALVKLVQQPQNVSTFINRPALGILPPENFVEKLRSLLSVAPKGM

PF AKKTLLVTTGSEA-----VENAVKIARATTGRAGVIAFT
EC AKKTLLVTTGSEAVENA-----VKIARAATKRSGTIAFS
HS -SQLITMACGSCSNENALKTIFMWYRSKERGQRGFSQEELETCMINQAPGCPDYSILSFM
JB -SQLITMACGSCSNENAFKTIFMWYRSKERGESAFSKEELETCMINQAPGCPDYSILSFM

PF GAYHRTMMTLGLTGKVVPYSAGMGLM--P-GGIFRALYPNELHGVS-V---DDSIAS-I
EC GAYHRTHYTLALTGKVNPYSAGMGL---MPGHVYRALYPCPLHGI---SEDDAIASI-
HS GAFHRTMGCLATTHSKAIHKIDIPSFDWPIAPFPRLKYPLEEFVKENQQEEARCLEEVE
JB GAFHRTMGCLATTHSKAIHKIDIPSFDWPIAPFPRLKYPLEEFVKENQQEEARCLEEVE

PF ERIFKNDAEPRDIAAIIIEPVQGEGGFYVAPKAFMKRLRELCDKHGILLIADEVQTGAGR
EC HRIFKNDAAPEDIAAIVIEPVQGEGGFYASSPAFMQRLRALCDEHGIMLIADEVQSGAGR
HS DLIVKYRKKKKTVAGIIVEPIQSEGGDNHASDDFFRKLRDIARKHGCAFLVDEVQTGGGC
JB DLIVKYRKKKKTVAGIIVEPIQSEGGDNHASDDFFRKLRDISRKHGCAFLVDEVQTGGGS

PF TGTFFAMEQMGVAA--DLTTFAKSI-AGGFPLAGVCGKAEYMDAIAPGGLGGTYAGSPIA
EC TGTLFAMEQMGVAP--DLTTFAKSI-AGGFPLAGVTGRAEVMDAVAPGGLGGTYAGNPIA
HS TGKFWAHEHWGLDDPADVMTFSKKMMTGGFFH----K-EEFRPNAPYRIFNTWLGDPSK
JB TGKFWAHEHWGLDDPADVMTFSKKMMTGGFFH----K-EEFRPNAPYRIFNTWLGDPSK

PF CAAALAVMEVFEEHLLDRCKAVGERLVTGLKAIQAKYPVI-GEVRALGAMIAELFEDG
EC CVAALEVLKVFEQENLLQKANDLGQKLKDGLLAIAEKHPEI-GDVRGLGAMIAIELFEDG
HS NLLLAEVINIIKREDLLNNAAHAGKALLTGLLDLQARYPQFISRVRGRGTFCSFDT----
JB NLLLAEVINIIKREDLLSNAAHAGKVLLTGLLDLQARYPQFISRVRGRGTFCSFDT----

PF DSHKPNAAAVASVVAKARDKGLILLSCGTYGNVLRVLVPLTSPDEQLDKGLAIIIECFSEL-
EC DHNKPDAKLTAEIVARARDKGLILLSCGPYYNVLRILVPLTIEDAQIRQGLEIISQCFDEAK
HS ----PDDSIRNKLLILIARNKGVVLGCGDKSIRFRPTLVFRDHHA--HLFLNIFSDILADFK
JB ----PDESIRNKLISIARNKGVMLGGCGDKSIRFRPTLVFRDHHA--HLFLNIFSDILADFK
```

Figure 41S. Alignment of *pseudomonas fluorescens* (PF), human (HS), *E. coli* (EC) and wild boar (JB). Red and blue color letters correspond to the residues of the chain A and chain B respectively, that interact with VGB 3 in the 1ohv crystal structure.

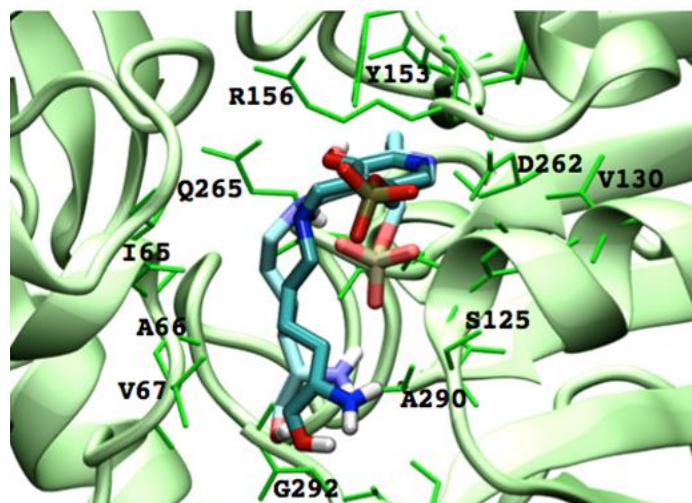


Figure 42S. Validation of the molecular docking calculation for the *pseudomonas* model. Ligand in the PDB:ID 3r4t crystal structure was reproduced with a RMSD of 1.7 Å. Ligand experimental (opaque color) and calculated conformation (shiny color) are displayed as sticks representation respectively. Residues within 4.0 Å of both ligands are shown as thin sticks.

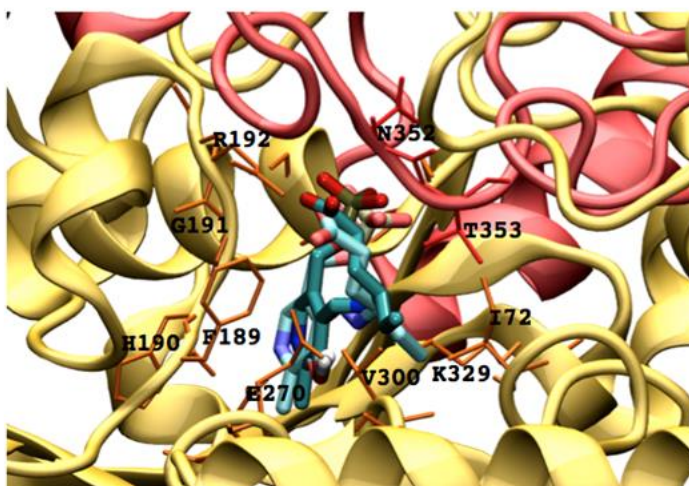


Figure 43S. Validation of the molecular docking calculation for the *human* model. Ligand in the PDB:ID 1ohw crystal structure was reproduced with a RMSD of 1.3 Å. Ligand experimental (opaque color) and calculated conformation (shiny color) are displayed as sticks representation respectively. Residues within 4.0 Å of both ligands are shown as thin sticks.

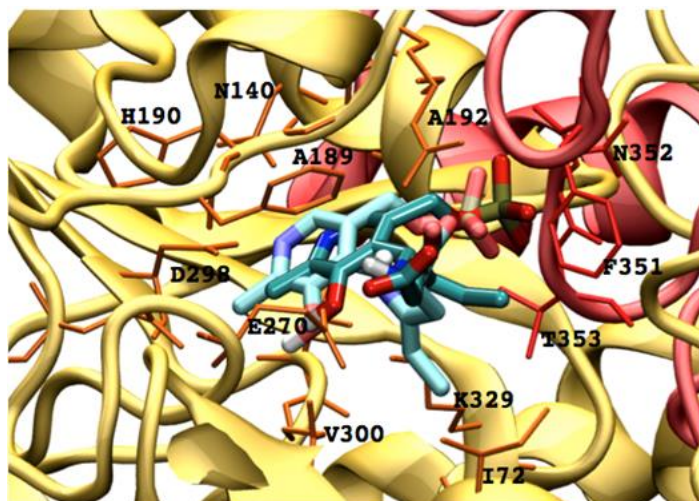


Figure 44S. Validation of the molecular docking calculation for the *human* model. Ligand in the PDB:ID 1ohy crystal structure was reproduced with a RMSD of 1.8 Å. Ligand experimental (opaque color) and calculated conformation (shiny color) are displayed as sticks representation respectively. Residues within 4.0 Å of both ligands are shown as thin sticks.

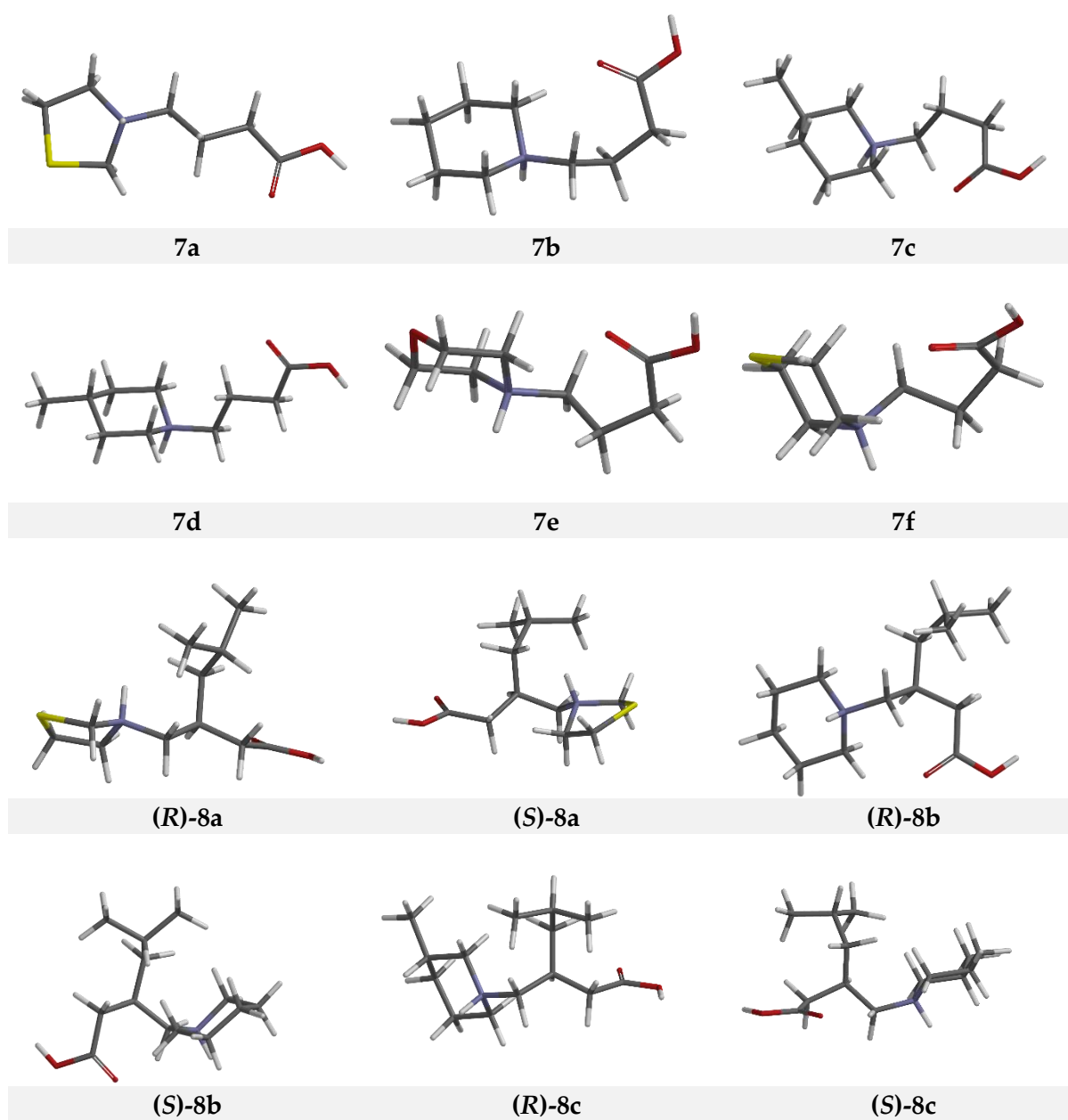


Figure 45S. Optimized structures of all GABA analogues, VPNa and VGB.

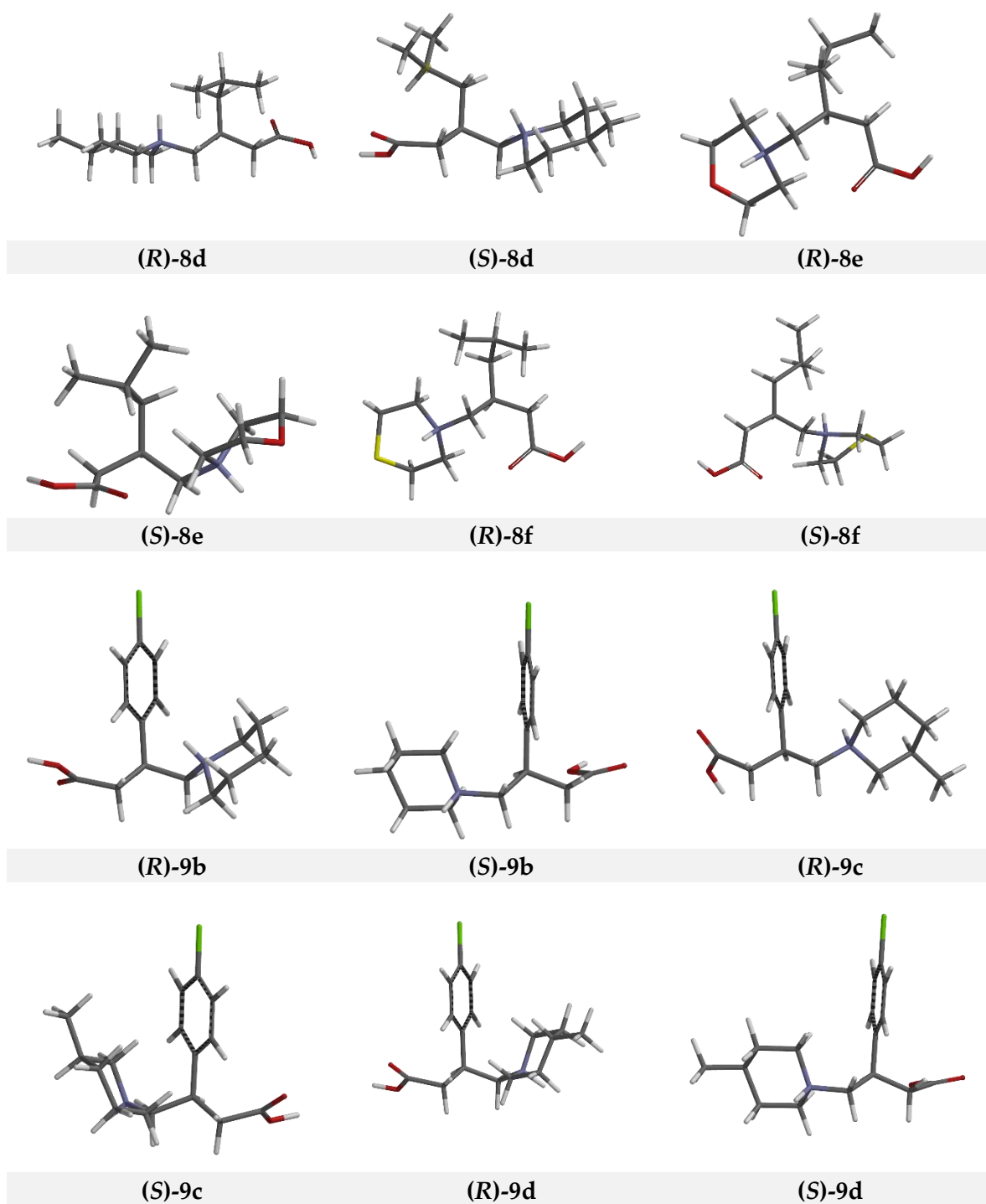


Figure 45S. Optimized structures of all GABA analogues, VPNa and VGB. Continuation

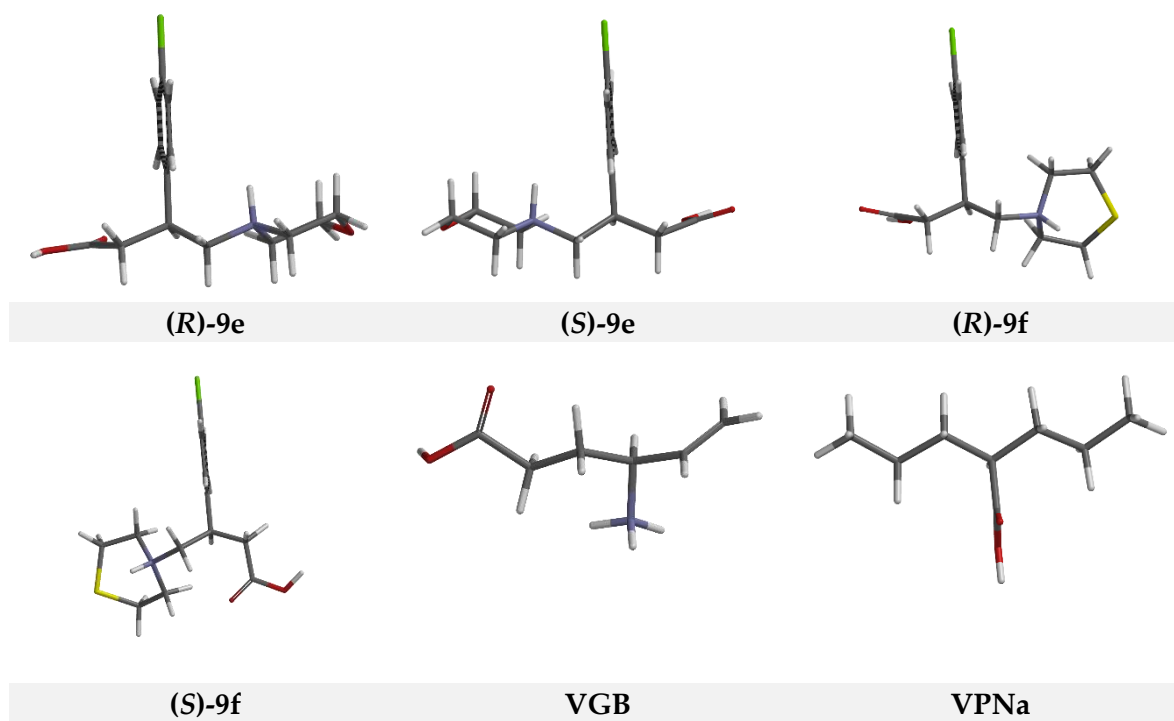


Figure 45S. Optimized structures of all GABA analogues, VPNa and VGB. Continuation

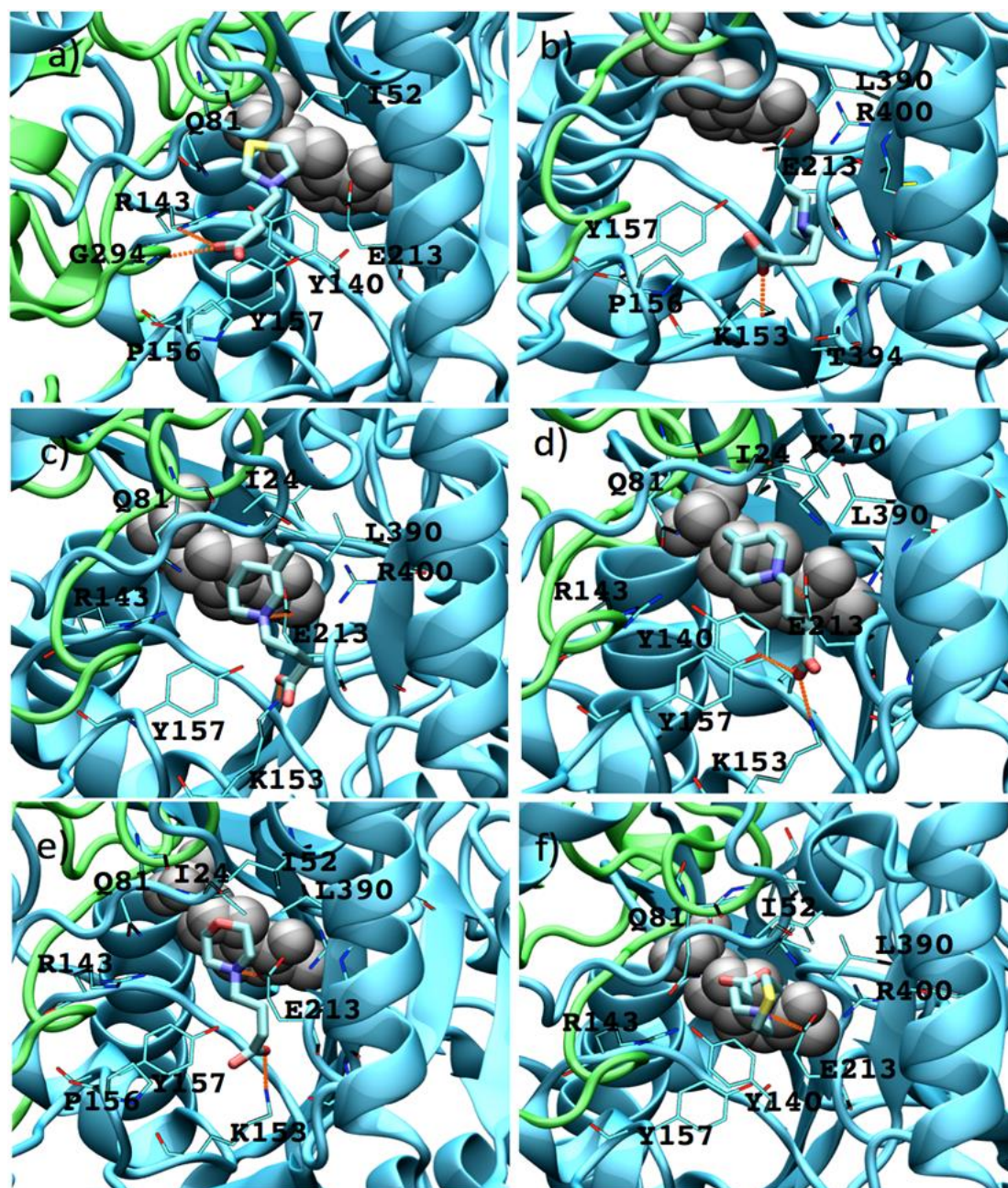
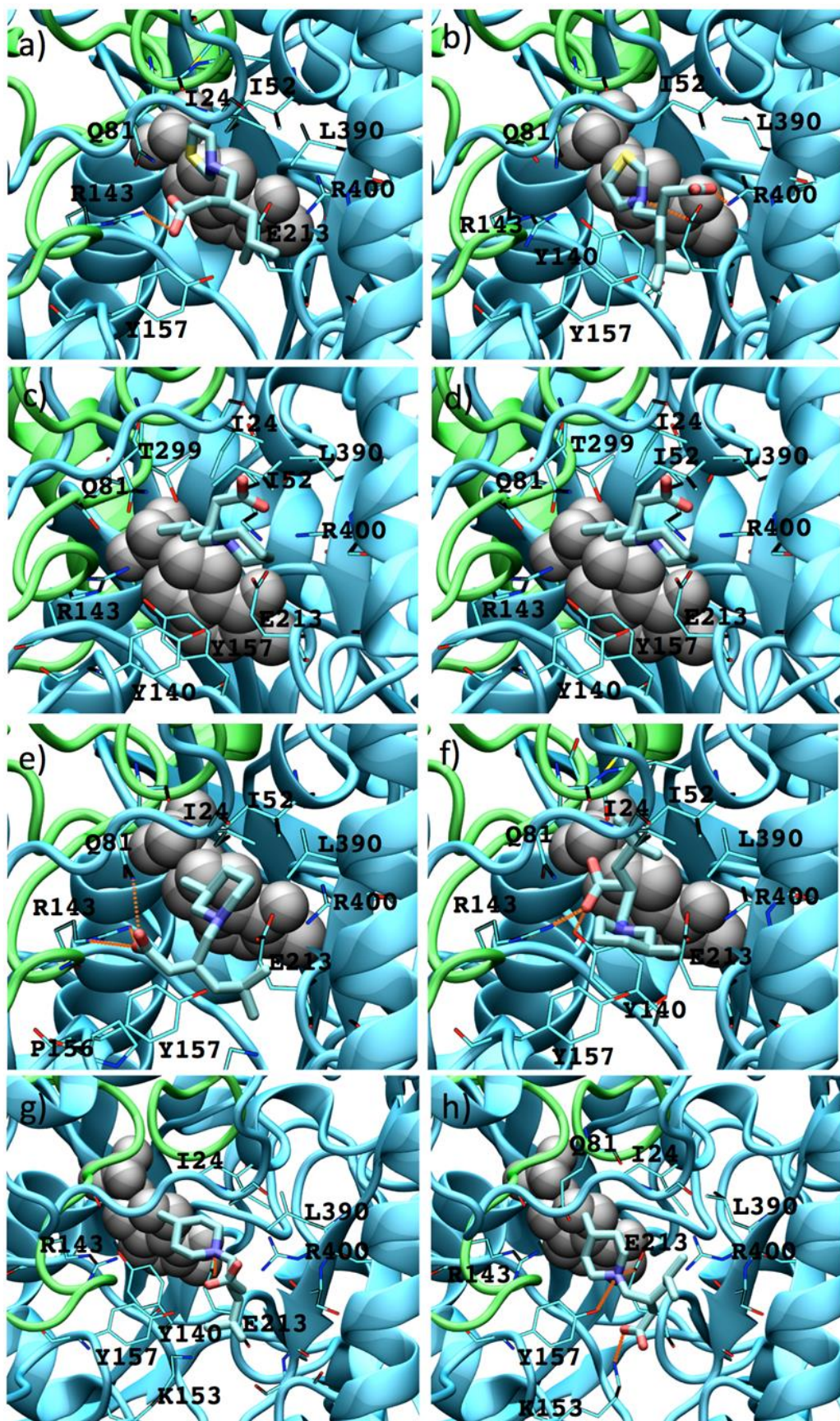


Figure 46S. Interactions between GABA analogues **7** and *Pseudomonas fluorescens* GABA-AT. a) **7a**, b) **7b**, c) **7c**, d) **7d**, e) **7e** and f) **7f**. PLP prosthetic group is showed as Van der Waals spheres and each protein chain is colored in green and cyan. Residues at 4 Å of each analogue are indicated. Hydrogen bonds are shown as orange dashed lines.



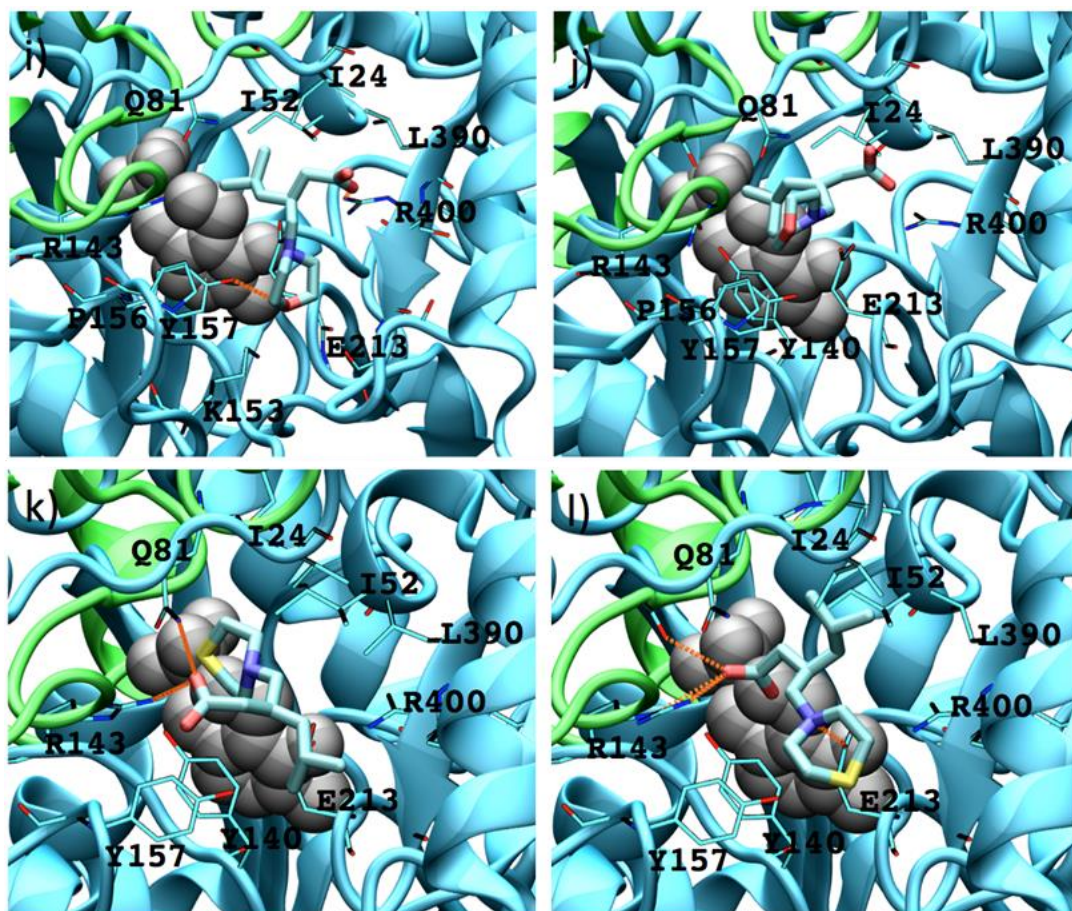


Figure 47S. Interactions between GABA analogues **8** and *Pseudomonas fluorescens* GABA-AT. a) (S)-**8a**, b) (R)-**8a**, c) (S)-**8b**, d) (R)-**8b**, e) (S)-**8c** and f) (R)-**8c**, g) (S)-**8d**, h) (R)-**8d**, i) (S)-**8e**, j) (R)-**8e**, k) (S)-**8f**, l) (R)-**8f**. PLP prosthetic group is shown as Van der Waals spheres and each protein chain is colored in green and cyan. Residues at 4 Å of each analogue are indicated. Hydrogen bonds are shown as orange dashed lines.

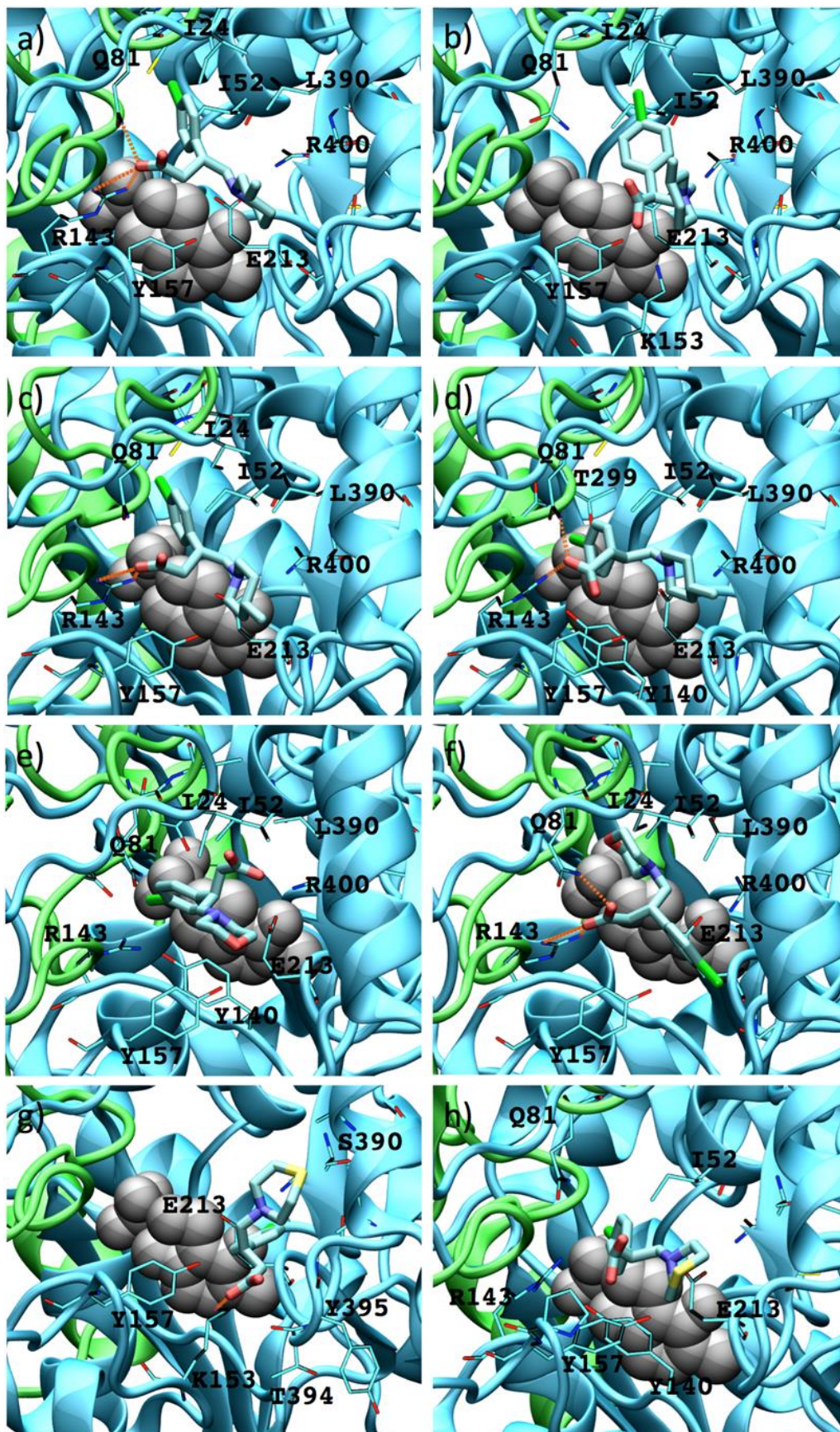


Figure 48S. Interactions between GABA analogues **9** and *Pseudomonas fluorescens* GABA-AT. a) (S)-**9c**, b) (R)-**9c**, c) (S)-**9d** and d) (R)-**9d**, e) (S)-**9e**, f) (R)-**9e**, g) (S)-**9f**, h) (R)-**9f**. PLP prosthetic group is showed as Van der Waals spheres and each protein chain is colored in green and cyan. Residues at 4 Å of each analogue are indicated. Hydrogen bonds are shown as orange dashed lines.

Table 1S. Energy interactions values obtained from the docking calculations of all GABA derivatives and *pseudomonas* GABA-AT model. All the values are in kcal/mol.

Ligand	MolDock Score	Electro	HBond
7a	-73.1062	-7.11035	-2.65911
7b	-69.4043	-3.21553	-7.4961
7c	-63.4051	-8.18821	-3.26379
7d	-88.9465	-5.28229	-5.17495
7e	-81.1331	-10.6664	-5.7402
7f	-82.0854	-9.3513	-8.95745
(S)- 8a	-88.4367	-7.59611	-2.37557
(R)- 8a	-80.2747	-4.34932	-1.54938
(S)- 8b	-95.13	-3.82411	-3.42391
(R)- 8b	-82.2497	-1.10123	-9.99797
(S)- 8c	-106.003	-11.4722	-6.60934
(R)- 8c	-84.4955	-2.78647	-5.59387
(S)- 8d	-102.496	-12.1057	-7.491
(R)- 8d	-79.0166	-7.77168	-3.27213
(S)- 8e	-97.1576	-7.49549	-4.62095
(R)- 8e	-85.5462	-5.56573	-1.57816
(S)- 8f	-110.456	-9.48398	-2.62015
(R)- 8f	-80.3773	-1.33976	-5.50014
(S)- 9b	-94.5623	-5.33333	-7.63276
(R)- 9b	-82.3833	-8.45774	-4.99611
(S)- 9c	-105.201	-4.4125	-6.8652
(R)- 9c	-92.4029	0.375594	-4.915
(S)- 9d	-93.087	-3.43971	-3.94599
(R)- 9d	-102.403	-5.70107	-3.30324
(S)- 9e	-97.4871	-4.61057	0
(R)- 9e	-90.7655	-4.02959	-8.75642
(S)- 9f	-92.252	-4.16681	-2.49799
(R)- 9f	-83.726	-0.300184	0
VPNa	-64.703	-5.43962	-6.16675

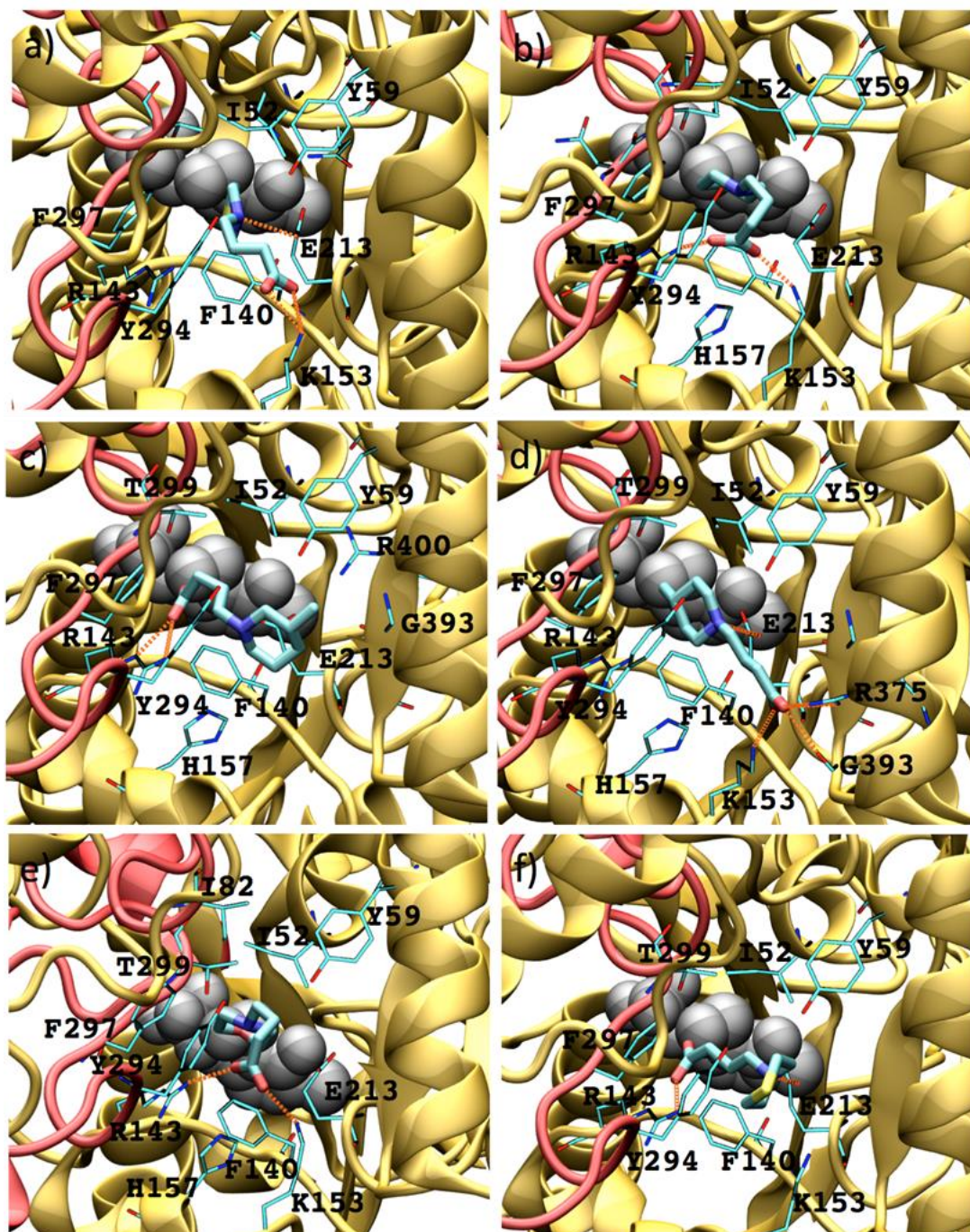
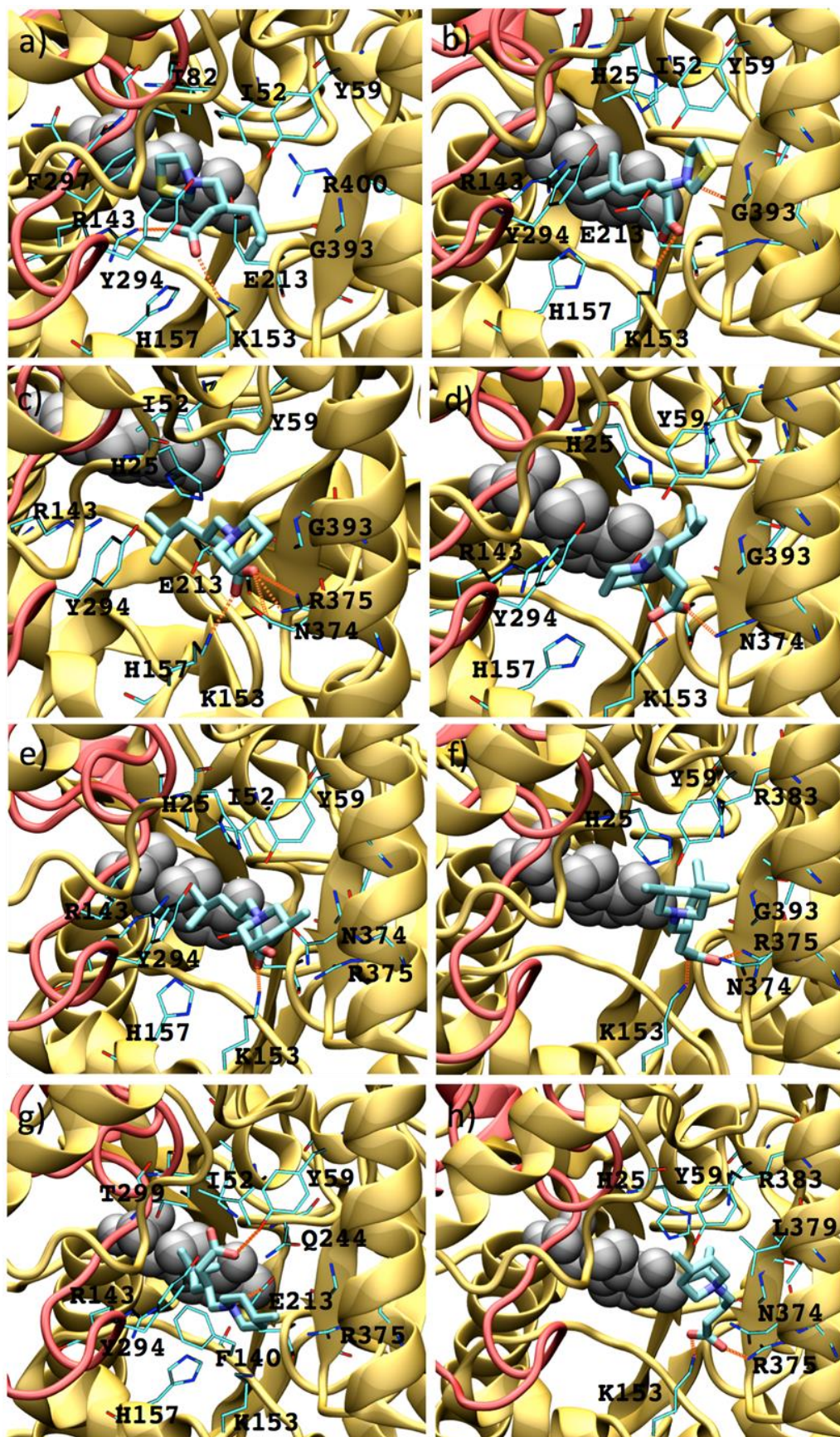


Figure 49S. Interactions between GABA analogues **7** and *Human* GABA-AT. a) **7a**, b) **7b**, c) **7c**, d) **7d**, e) **7e** and f) **7f**. PLP prosthetic group is shown as Van der Waals spheres and each protein chain is colored in yellow and red. Residues at 4 Å of each analogue are indicated. Hydrogen bonds are shown as orange dashed lines.



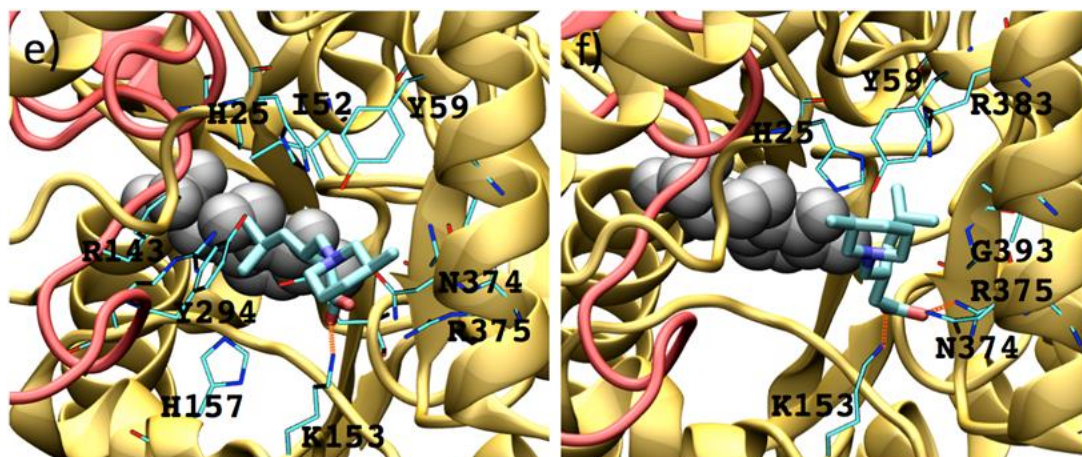
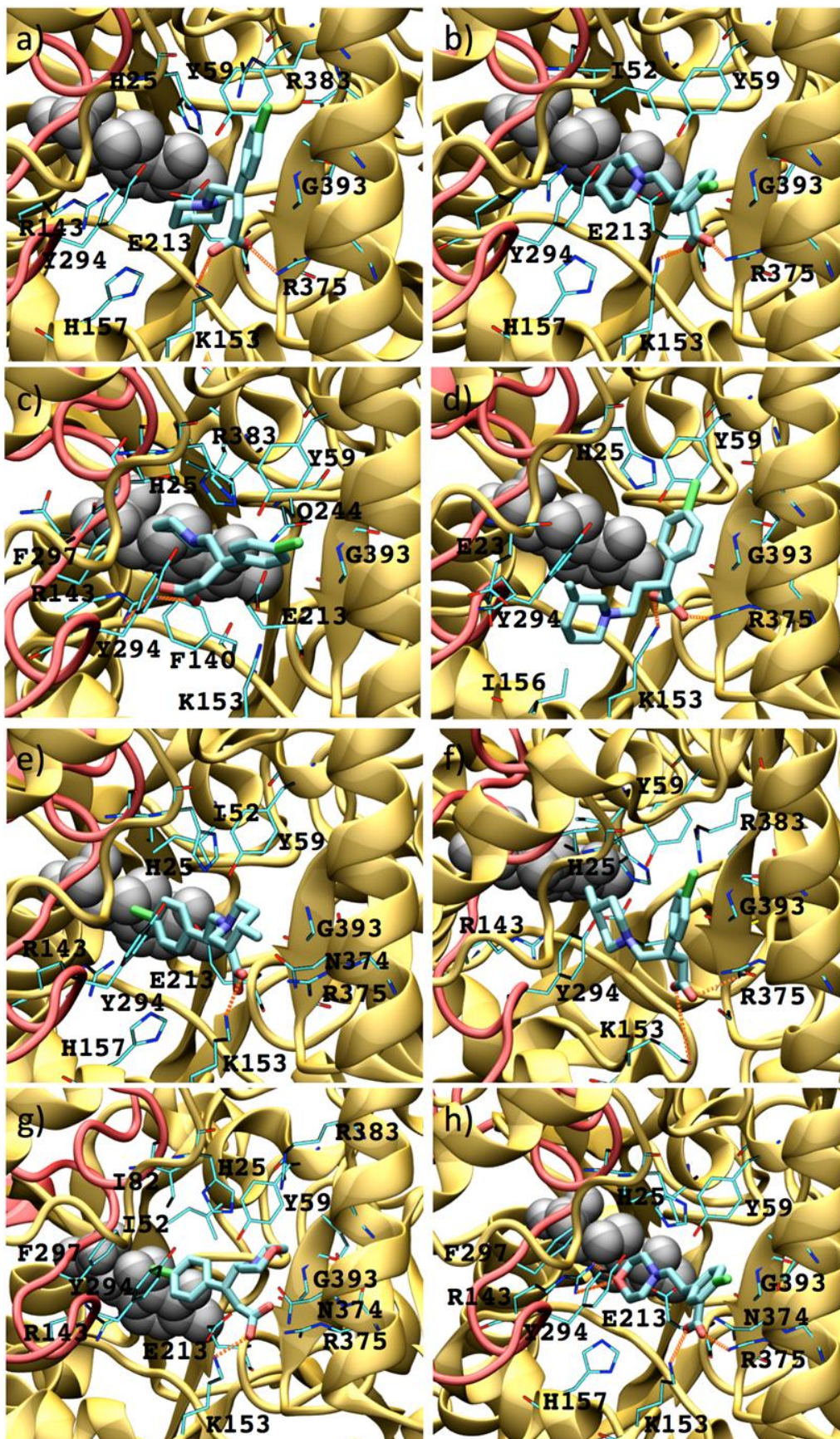


Figure 50S. Interactions between GABA analogues **8** and *Human* GABA-AT. a) (*S*)-**8a**, b) (*R*)-**8a**, c) (*S*)-**8b**, d) (*R*)-**8b**, e) (*S*)-**8c** and f) (*R*)-**8c**, g) (*S*)-**8d**, h) (*R*)-**8d**, i) (*S*)-**8e**, j) (*R*)-**8e**, k) (*S*)-**8f**, l) (*R*)-**8f**. PLP prosthetic group is showed as Van der Waals spheres and each protein chain is colored in yellow and red. Residues at 4 Å of each analogue are indicated. Hydrogen bonds are shown as orange dashed lines.



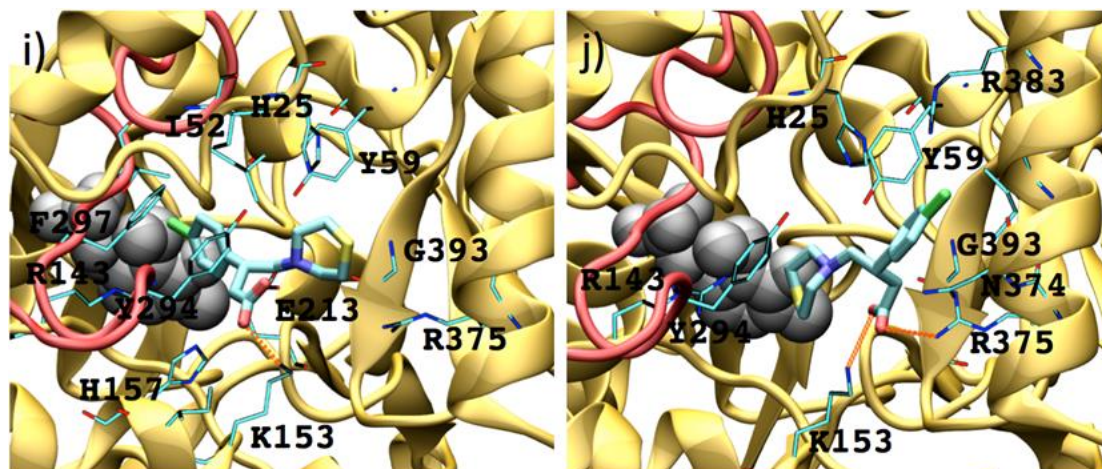


Figure 51S. Interactions between GABA analogues **9** and *Human* GABA-AT. a) (*S*)-**9b**, b) (*R*)-**9b**, c) (*S*)-**9c** and d) (*R*)-**9c**, e) (*S*)-**9d**, f) (*R*)-**9d**, g) (*S*)-**9e**, h) (*R*)-**9e**, i) (*S*)-**9f**, j) (*R*)-**9f**. PLP prosthetic group is showed as Van der Waals spheres and each protein chain is colored in yellow and red. Residues at 4 Å of each analogue are indicated. Hydrogen bonds are shown as orange dashed lines.

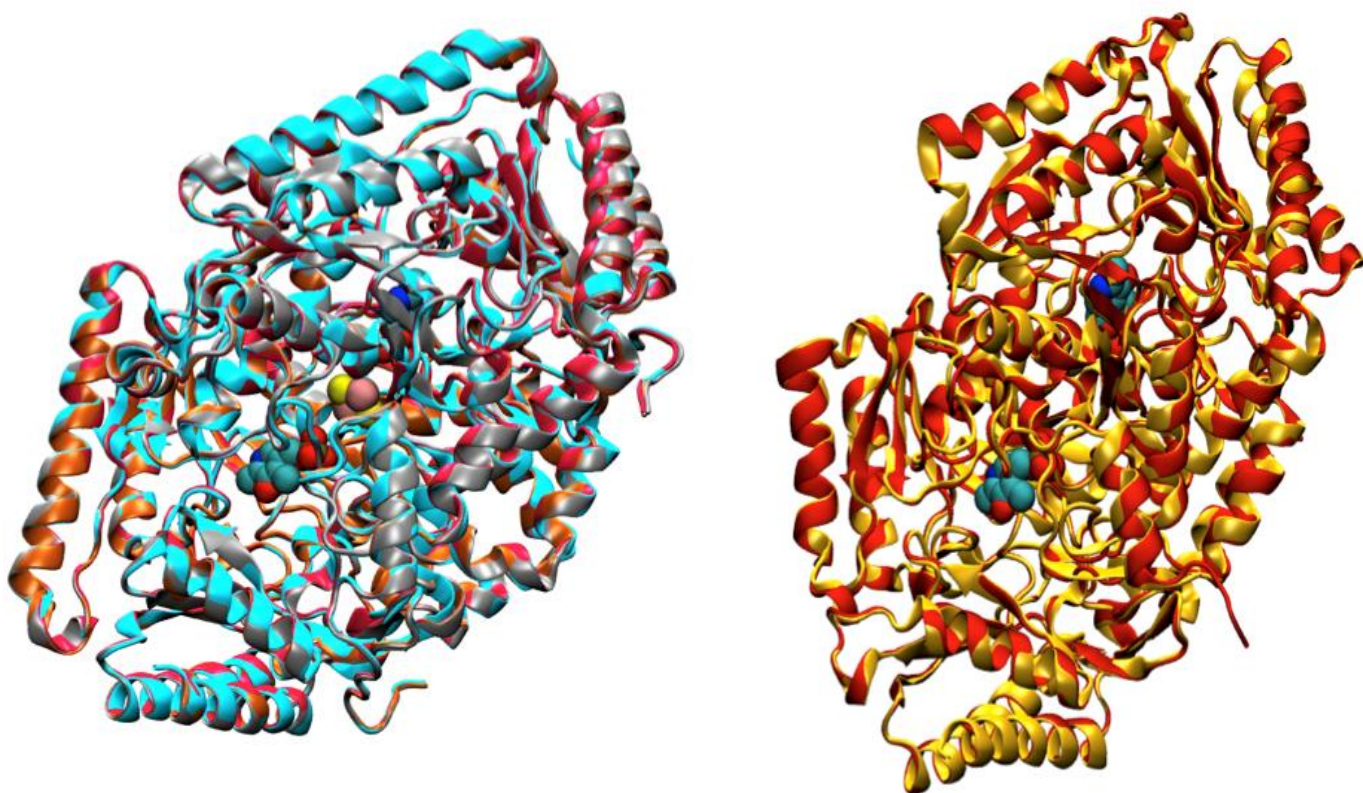


Figure 52S. Backbone structural alignment of GABA-AT structures. a) GABA-AT human model in cyan color. **1ohv**, **1ohw** and **1ohy** *Sus scrofa* crystal structures in red (RMSD=0.35), gray (RMSD=0.36) and orange (RMSD=0.40) color respectively. b) GABA-AT *Pseudomonas fluorescens* model in shiny red color, **1sf2** *E. coli* structure in shiny yellow color (RMSD= 0.52). Fe₂S₂ (yellow/pink color) and PLP from human model in VDW representation.

Table 2S. Energy interactions values obtained from the docking calculations of all GABA derivatives and *human* GABA-AT model. All the values are in kcal/mol.

Ligand	MolDock Score	Electro	HBond
7a	-73.7827	-11.6791	-6.37482
7b	-90.0906	-14.3794	-2.70548
7c	-87.1437	-4.79249	-4.66131
7d	-93.3451	-16.3569	-7.2265
7e	-101.729	-10.9936	-4.12353
7f	-83.6899	-11.9784	-3.44067
(S)-8a	-112.119	-7.99459	-3.85277
(R)-8a	-97.5094	-6.93326	-3.08695
(S)-8b	-98.5854	-11.0659	-5.84991
(R)-8b	-93.2925	-12.0228	-1.80199
(S)-8c	-113.181	-7.06026	-2.5
(R)-8c	-89.7572	-13.2412	-3.34681
(S)-8d	-107.919	-2.81265	-4.36016
(R)-8d	-93.1624	-5.66396	-2.5
(S)-8e	-111.347	-2.23916	-0.215018
(R)-8e	-103.812	-14.4581	-3.64372
(S)-8f	-105.834	-13.386	-2.83697
(R)-8f	-89.8468	-13.3805	-2.49901
(S)-9b	-100.144	-8.84278	-3.14615
(R)-9b	-95.7124	-11.0181	-2.4786
(S)-9c	-105.791	-11.6063	-2.11356
(R)-9c	-91.5724	-8.52886	-3.78333
(S)-9d	-107.209	-10.6489	-2.5
(R)-9d	-98.4869	-10.3527	-3.17113
(S)-9e	-109.605	-9.38255	-2.5
(R)-9e	-112.69	-10.5368	-8.05182
(S)-9f	-122.362	-10.3354	-2.5
(R)-9f	-103.599	-9.33766	-2.4934
VPNa	-73.7153	-7.61745	0

Table 3S. Values of the experimental (Y_{Exp}), calculated (Y_{Cal}) and predicted (Y_{Pred}) percent of inhibition of the GABA derivatives. Compounds that were considered form the test validation are marked with a script symbol.

Mol	Y _{Calc1}	Y _{Pred1}	Y _{Calc2}	Y _{Pred2}	Y _{Calc3}	Y _{Pred3}	Y _{Calc4}	Y _{Pred4}	Y _{Calc5}	Y _{Pred5}	Y _{Calc6}	Y _{Pred6}	Y _{Calc7}	Y _{Pred7}	Y _{Calc8}	Y _{Pred8}	Y _{Calc9}	Y _{Pred9}	Y _{Calc10}	Y _{Pred10}	Y _{Exp}
7a	25.68	26	-	26.91	25.79	26.19	-	26.18	24.28	23.97	23.71	23.19	25.33	25.52	-	25.84	-	27.67	-	25.35	24.9
7b	19.65	18.12	20.76	19.59	20.43	19.15	20.19	19.06	19.9	18.33	21.19	20.34	20.47	19.07	20.67	19.4	21.29	19.88	20.11	18.62	24.9
7c	20.39	20.7	21.49	22.13	-	21.14	20.78	21.14	20.59	21.01	21.92	22.54	21.14	21.73	21.39	22.03	-	22.05	20.8	21.27	19.4
7d	-	21.45	22.55	22.42	22.17	21.92	21.65	21.28	-	21.59	22.99	23.01	-	22.12	22.42	22.25	23.16	23.29	-	21.8	22.9
7e	19.65	20.05	20.76	21.45	20.43	21.04	20.19	20.64	19.9	20.41	21.19	21.85	20.47	21.15	-	20.67	21.29	22.46	20.11	20.67	18.3
7f	28.54	29.91	-	29.8	28.51	29.96	28.67	30.88	26.79	27.01	26.08	25.8	27.87	28.87	28.54	30.86	-	30.67	27.99	29.65	26.5
8a	0.81	4.52	2.05	5.81	1.59	5.43	-	5.91	-	0.95	-1.26	1.59	2.39	6.86	1.52	5.24	1.82	5.33	1.9	5.54	-3.5
8b	0.16	-0.12	1.27	1.47	1.46	1.66	4.29	5.94	1.62	2	1.62	1.91	2.49	3.11	1.61	1.85	1.03	1.1	1.73	2.06	0.84
8c	5.87	5.85	-	6.97	7.01	7.22	8.95	9.64	6.97	7.19	7.35	7.63	7.75	8.17	7.19	7.41	6.96	7.14	-	7.11	5.96
8d	6.93	7.88	8.03	9.08	8.04	9.03	-	9.81	7.96	9	-	8.41	-	8.73	8.22	9.18	8.06	8.97	8.11	9.2	2.64
8e	-	0.16	1.27	-0.99	1.46	-0.06	4.29	3.39	1.62	-0.64	1.62	-0.09	2.49	1.08	1.61	0.17	1.03	-0.9	1.73	0.06	6.2
8f	9.05	5.27	10.31	5.81	9.54	5.85	12.78	9.08	-	8.5	-	6.51	9.89	6.39	9.48	5.49	10.4	5.94	9.61	6.31	16.8
9b*	-	-	-	-	-	-	-	-	-	-	-	-	-	-	-	-	-	-	-	-	73
9c	-	26.19	27.89	25.5	27.99	12.55	27.69	20.73	28.12	31.25	28.07	52.09	28.17	35.81	-	28.34	27.9	25.78	27.98	27.46	28
9d	9.21	18.37	8.87	9.17	-	7.64	8.12	7.55	9.23	10.15	-	11.64	9.26	10.4	9.08	16.37	8.96	9.38	8.94	9.34	8.6
9e	5.14	3.56	5.21	4.03	-	4.45	5.95	5.37	6	5.48	7.43	8.27	6.16	5.54	5.63	4.41	4.99	3.68	5.71	5	7
9f	15.45	18.65	15.83	17.97	14.21	29.61	16.04	17.9	14.45	14.81	13.7	13.01	-	15.13	15.09	17.44	15.94	18.12	15.17	16.05	14.2
VPNa*	-	-	-	-	-	-	-	-	-	-	-	-	-	-	-	-	-	-	-	-	40

* Molecules considered as outliers.

- Compounds considered for the test validation.